

2 **The protonmotive force and respiratory control:**

3 **Building blocks of mitochondrial physiology**

4 **Part 1.**

5 http://www.mitoeagle.org/index.php/MitoEAGLE_preprint_2017-09-21

6 Preprint version 14 (2017-11-01)

7
8 **MitoEAGLE Network**

9 Corresponding author: Gnaiger E

10 Contributing co-authors

11 Ahn B, Alves MG, Amati F, Åsander Frostner E, Bailey DM, Bastos Sant'Anna Silva AC,
12 Battino M, Beard DA, Ben-Shachar D, Bishop D, Breton S, Brown GC, Brown RA, Buettner
13 GR, Carvalho E, Cervinkova Z, Chang SC, Chicco AJ, Coen PM, Collins JL, Crisóstomo L,
14 Davis MS, Dias T, Distefano G, Doerrier C, Ehinger J, Elmer E, Fell DA, Ferko M, Ferreira
15 JCB, Filipovska A, Fisher J, Garcia-Roves PM, Garcia-Souza LF, Genova ML, Gonzalo H,
16 Goodpaster BH, Gorr TA, Han J, Harrison DK, Hellgren KT, Hernansanz P, Holland O,
17 Hoppel CL, Iglesias-Gonzalez J, Irving BA, Iyer S, Jackson CB, Jansen-Dürr P, Jespersen
18 NR, Jha RK, Kaambre T, Kane DA, Kappler L, Keijer J, Komlodi T, Kopitar-Jerala N, Krako
19 Jakovljevic N, Kuang J, Labieniec-Watala M, Lai N, Laner V, Lee HK, Lemieux H, Lerfall J,
20 Lucchinetti E, MacMillan-Crow LA, Makrecka-Kuka M, Meszaros AT, Moiso N, Molina
21 AJA, Montaigne D, Moore AL, Murray AJ, Newsom S, Nozickova K, O'Gorman D, Oliveira
22 PF, Oliveira PJ, Orynbayeva Z, Pak YK, Palmeira CM, Patel HH, Pesta D, Petit PX, Pichaud
23 N, Pirkmajer S, Porter RK, Pranger F, Prochownik EV, Radenkovic F, Reboredo P, Renner-
24 Sattler K, Robinson MM, Rohlena J, Røslund GV, Rossiter HB, Salvadego D, Scatena R,
25 Schartner M, Scheibye-Knudsen M, Schilling JM, Schlattner U, Schoenfeld P, Scott GR,
26 Singer D, Sobotka O, Spinazzi M, Stier A, Stocker R, Sumbalova Z, Suravajhala P, Tanaka

27 M, Tandler B, Tepp K, Tomar D, Towheed A, Trivigno C, Tronstad KJ, Trougakos IP,
28 Tyrrell DJ, Velika B, Vendelin M, Vercesi AE, Victor VM, Ward ML, Watala C, Wei YH,
29 Wieckowski MR, Wohlwend M, Wolff J, Wuest RCI, Zaugg K, Zaugg M, Zorzano A

30

31 Supporting co-authors:

32 Arandarčikaitė O, Bakker BM, Bernardi P, Boetker HE, Borsheim E, Borutaitė V, Bouitbir J,
33 Calabria E, Calbet JA, Chaurasia B, Clementi E, Coker RH, Collin A, Das AM, De Palma C,
34 Dubouchaud H, Duchon MR, Durham WJ, Dyrstad SE, Engin AB, Fornaro M, Gan Z, Garlid
35 KD, Garten A, Gourlay CW, Granata C, Haas CB, Haavik J, Haendeler J, Hand SC, Hepple
36 RT, Hickey AJ, Hoel F, Kainulainen H, Keppner G, Khamoui AV, Klingenspor M, Koopman
37 WJH, Kowaltowski AJ, Krajcova A, Lenaz G, Malik A, Markova M, Mazat JP, Menze MA,
38 Methner A, Muntané J, Muntean DM, Neuzil J, Oliveira MT, Pallotta ML, Parajuli N,
39 Pettersen IKN, Porter C, Pulinilkunnit T, Ropelle ER, Salin K, Sandi C, Sazanov LA,
40 Siewiera K, Silber AM, Skolik R, Smenes BT, Soares FAA, Sokolova I, Sonkar VK,
41 Stankova P, Swerdlow RH, Szabo I, Trifunovic A, Thyfault JP, Tretter L, Vieyra A, Votion

42 DM, Williams C

43

44 **Updates:**

45 http://www.mitoeagle.org/index.php/MitoEAGLE_preprint_2017-09-21

46

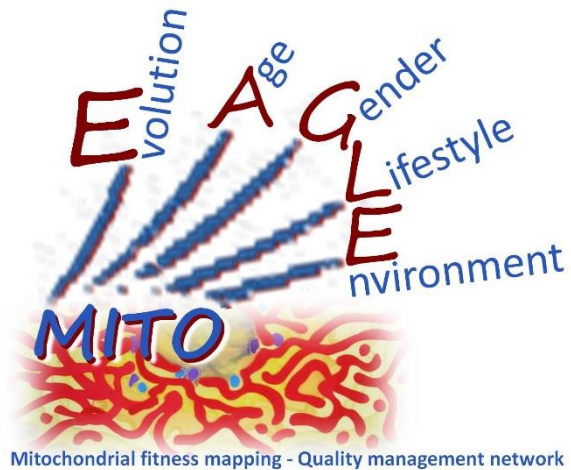
Correspondence: Gnaiger E

Department of Visceral, Transplant and Thoracic Surgery, D. Swarovski Research Laboratory, Medical University of Innsbruck, Innrain 66/4, A-6020 Innsbruck, Austria

Email: erich.gnaiger@i-med.ac.at

Tel: +43 512 566796, Fax: +43 512 566796 20

This manuscript on 'The protonmotive force and respiratory control' is a position statement in the frame of COST Action CA15203 MitoEAGLE. The list of co-authors evolved from MitoEAGLE Working Group Meetings and a **bottom-up** spirit of COST in phase 1: This is an open invitation to scientists and students to join as co-authors, to provide a balanced view on mitochondrial respiratory control, a fundamental introductory presentation of the concept of the protonmotive force, and a consensus statement on reporting data of mitochondrial respiration in terms of metabolic flows and fluxes. We plan a series of follow-up reports by the expanding MitoEAGLE Network, to increase the scope of recommendations on harmonization and facilitate global communication and collaboration.



Phase 2: MitoEAGLE preprint (Versions 01 – 10): We continue to invite comments and suggestions on the, particularly if you are an **early career investigator adding an open future-oriented perspective**, or an **established scientist providing a balanced historical basis**. Your critical input into the quality of the manuscript will be most welcome, improving our aims to be educational, general, consensus-oriented, and practically helpful for students working in mitochondrial respiratory physiology.

Phase 3 (2017-11-11): Manuscript submission to a preprint server, such as BioRxiv. We want to invite further opinion leaders: To join as a co-author, please feel free to focus on a particular section in terms of direct input and references, contributing to the scope of the manuscript from the perspective of your expertise. Your comments will be largely posted on the discussion page of the MitoEAGLE preprint website.

If you prefer to submit comments in the format of a referee's evaluation rather than a contribution as a co-author, I will be glad to distribute your views to the updated list of co-authors for a balanced response. We would ask for your consent on this open bottom-up policy.

Phase 4: We organize a MitoEAGLE session linked to our series of reports at the MiPconference Nov 2017 in Hradec Kralove in close association with the MiP society (where you hopefully will attend) and at EBEC 2018 in Budapest.

» http://www.mitoeagle.org/index.php/MiP2017_Hradec_Kralove_CZ

I thank you in advance for your feedback.

With best wishes,

Erich Gnaiger

Chair Mitochondrial Physiology Society - <http://www.mitophysiology.org>

Chair COST Action MitoEAGLE - <http://www.mitoeagle.org>

Medical University of Innsbruck, Austria

97	Contents
98	1. Introduction
99	2. Respiratory coupling states in mitochondrial preparations
100	Mitochondrial preparations
101	2.1. <i>Three coupling states of mitochondrial preparations and residual oxygen consumption</i>
102	Coupling control states and respiratory capacities
103	Kinetic control
104	Phosphorylation, P_{\gg}
105	LEAK, OXPHOS, ET, ROX
106	2.2. <i>Coupling states and respiratory rates</i>
107	2.3. <i>Classical terminology for isolated mitochondria</i>
108	States 1-5
109	3. The protonmotive force and proton flux
110	3.1. <i>Electric and chemical partial forces versus electrical and chemical units</i>
111	Faraday constant
112	Electric part of the protonmotive force
113	Chemical part of the protonmotive force
114	3.2. <i>Definitions</i>
115	Control and regulation
116	Respiratory control and response
117	Respiratory coupling control
118	Pathway control states
119	The steady-state
120	3.3. <i>Forces and fluxes in physics and irreversible thermodynamics</i>
121	Vectorial and scalar forces, and fluxes
122	Coupling
123	Coupled versus bound processes
124	4. Normalization: fluxes and flows
125	4.1. <i>Flux per chamber volume</i>
126	4.2. <i>System-specific and sample-specific normalization</i>
127	Extensive quantities
128	Size-specific quantities
129	Molar quantities
130	Flow per system, I
131	Size-specific flux, J
132	Sample concentration, C_{mX}
133	Mass-specific flux, J_{mX,O_2}
134	Number concentration, C_{NX}
135	Flow per sample entity, I_{X,O_2}
136	4.3. <i>Normalization for mitochondrial content</i>
137	Mitochondrial concentration, C_{mte} , and mitochondrial markers
138	Mitochondria-specific flux, J_{mte,O_2}
139	4.4. <i>Conversion: units and normalization</i>
140	4.5. <i>Conversion: oxygen, proton and ATP flux</i>
141	5. Conclusions
142	6. References
143	

144 **Abstract**

145 Clarity of concept and consistency of nomenclature are key trademarks of a research field.
146 These trademarks facilitate effective transdisciplinary communication, education, and
147 ultimately further discovery. As the knowledge base and importance of mitochondrial
148 physiology to human health expand, the necessity for harmonizing nomenclature concerning
149 mitochondrial respiratory states and rates has become increasingly apparent. Peter Mitchell's
150 concept of the protonmotive force establishes the links between electrical and chemical
151 components of energy transformation and coupling in oxidative phosphorylation. This unifying
152 concept provides the framework for developing a consistent nomenclature for mitochondrial
153 physiology and bioenergetics. Herein, we follow IUPAC guidelines on general terms of
154 physical chemistry, extended by the concepts of open systems and irreversible thermodynamics.
155 We align the nomenclature of classical bioenergetics on respiratory states with a concept-driven
156 constructive terminology to address the meaning of each respiratory state. Furthermore, we
157 suggest uniform standards for the evaluation of respiratory states that will ultimately support
158 the development of databases of mitochondrial respiratory function in species, tissues and cells
159 studied under diverse physiological and experimental conditions. In this position statement, in
160 the frame of COST Action CA15203 MitoEAGLE, we endeavour to provide a balanced view
161 on mitochondrial respiratory control, a fundamental introductory presentation of the concept of
162 the protonmotive force, and a critical discussion on reporting data of mitochondrial respiration
163 in terms of metabolic flows and fluxes.

164

165 *Keywords:* Mitochondrial respiratory control, coupling control, mitochondrial
166 preparations, protonmotive force, chemiosmotic theory, oxidative phosphorylation, OXPHOS,
167 efficiency, electron transfer, ET; proton leak, LEAK, residual oxygen consumption, ROX, State
168 2, State 3, State 4, normalization, flow, flux

169

170

171 **Box 1:**

172

173 **In brief:**174 **mitochondria**175 **and Bioblasts**

- * Does the public expect biologists to understand Darwin's theory of evolution?
- * Do students expect that researchers of bioenergetics can explain Mitchell's theory of chemiosmotic energy transformation?

176 **Mitochondria** were described for the first time in 1857 by Rudolph Albert Kölliker as granular177 structures or 'sarkosomes' *(a reference is needed)*. In 1886 *(a reference is needed)* Richard

178 Altmann called them 'bioblasts' (published 1894). The word 'mitochondrium' (Greek mitos:

179 thread; chondros: granule) was introduced by Carl Benda (1898). Mitochondria are the oxygen

180 consuming electrochemical generators which evolved from endosymbiotic bacteria (Margulis

181 1970; Lane 2005). The bioblasts of Richard Altmann (1894) included not only the mitochondria

182 as presently defined, but also symbiotic and free-living bacteria.

183 We now recognize mitochondria as dynamic organelles with a double membrane that are

184 contained within eukaryotic cells. The mitochondrial inner membrane (mtIM) shows dynamic

185 tubular to disk-shaped cristae that separate the mitochondrial matrix, *i.e.* the internal

186 mitochondrial compartment, and the intermembrane space; the latter being enclosed by the

187 mitochondrial outer membrane (mtOM). Mitochondria are the structural and functional

188 elemental units of cell respiration. Cell respiration is the consumption of oxygen by electron

189 transfer coupled to electrochemical proton translocation across the mtIM. In the process of

190 oxidative phosphorylation (OXPHOS), the reduction of O₂ is electrochemically coupled to the

191 transformation of energy in the form of adenosine triphosphate (ATP; Mitchell 1961, 2011).

192 These powerhouses of the cell contain the machinery of the OXPHOS-pathway, including

193 transmembrane respiratory complexes (*i.e.* proton pumps with FMN, Fe-S and cytochrome *b*,
194 *c*, *aa₃* redox systems); alternative dehydrogenases and oxidases; the coenzyme ubiquinone (Q);

195 ATP synthase; the enzymes of the tricarboxylic acid cycle and the fatty acid oxidation enzymes;

196 transporters of ions, metabolites and co-factors; and mitochondrial kinases related to energy

197 transfer pathways. The mitochondrial proteome comprises over 1,200 proteins

198 (MITOCARTA), mostly encoded by nuclear DNA (nDNA), with a variety of functions, many
199 of which are relatively well known (*e.g.* apoptosis-regulating proteins), while others are still
200 under investigation, or need to be identified (*e.g.* alanine transporter).

201 Mitochondria typically maintain several copies of their own genome (hundred to
202 thousands per cell; Cummins 1998), which is almost exclusively maternally inherited (White *et*
203 *al.* 2008) and known as mitochondrial DNA (mtDNA). One exception to strictly maternal
204 inheritance in animals is found in bivalves (Breton *et al.* 2007). mtDNA is 16.5 Kb in length,
205 contains 13 protein-coding genes for subunits of the transmembrane respiratory Complexes CI,
206 CIII, CIV and ATP synthase, and also encodes 22 tRNAs and the mitochondrial 16S and 12S
207 rRNA. The mitochondrial genome is both regulated and supplemented by nuclear-encoded
208 mitochondrial targeted proteins. Evidence has accumulated that additional gene content is
209 encoded in the mitochondrial genome, *e.g.* microRNAs, piRNA, smithRNAs, repeat associated
210 RNA, and even additional proteins (Duarte *et al.* 2014; Lee *et al.* 2015; Cobb *et al.* 2016).

211 The mtIM contains the non-bilayer phospholipid cardiolipin, which is not present in any
212 other eukaryotic cellular membrane. Cardiolipin promotes the formation of respiratory
213 supercomplexes, which are supramolecular assemblies based upon specific, though dynamic,
214 interactions between individual respiratory complexes (Greggio *et al.* 2017; Lenaz *et al.* 2017).
215 Membrane fluidity is an important parameter influencing functional properties of proteins
216 incorporated in the membranes (Waczulikova *et al.* 2007). There is a constant crosstalk between
217 mitochondria and the other cellular components, maintaining cellular mitostasis through
218 regulation at both the transcriptional and post-translational level, and through cell signalling
219 including proteostatic (*e.g.* the ubiquitin-proteasome and autophagy-lysosome pathways) and
220 genome stability modules throughout the cell cycle or even cell death, contributing to
221 homeostatic regulation in response to varying energy demands and stress (Quiros *et al.* 2016).
222 In addition to mitochondrial movement along the microtubules, mitochondrial morphology can
223 change in response to the energy requirements of the cell via processes known as fusion and

224 fission, through which mitochondria can communicate within a network, and in response to
225 intracellular stress factors causing swelling and ultimately permeability transition.

226 Mitochondrial dysfunction is associated with a wide variety of genetic and degenerative
227 diseases. Robust mitochondrial function is supported by physical exercise and caloric balance,
228 and is central for sustained metabolic health throughout life. Therefore, a better understanding
229 of mitochondrial physiology will improve our understanding of the etiology of disease, the
230 diagnostic repertoire of mitochondrial medicine, with a focus on protective medicine, lifestyle
231 and healthy aging.

232 Abbreviation: mt, as generally used in mtDNA. Mitochondrion is singular and
233 mitochondria is plural.

234 *‘For the physiologist, mitochondria afforded the first opportunity for an experimental*
235 *approach to structure-function relationships, in particular those involved in active transport,*
236 *vectorial metabolism, and metabolic control mechanisms on a subcellular level’ (Ernster and*
237 *Schatz 1981).*

238

239 **1. Introduction**

240 Mitochondria are the powerhouses of the cell with numerous physiological, molecular,
241 and genetic functions (**Box 1**). Every study of mitochondrial function and disease is faced with
242 **E**volution, **A**ge, **G**ender and sex, **L**ifestyle, and **E**nvironment (EAGLE) as essential background
243 conditions intrinsic to the individual patient or subject, cohort, species, tissue and to some extent
244 even cell line. As a large and highly coordinated group of laboratories and researchers, the
245 mission of the global MitoEAGLE Network is to generate the necessary scale, type, and quality
246 of consistent data sets and conditions to address this intrinsic complexity. Harmonization of
247 experimental protocols and implementation of a quality control and data management system
248 is required to interrelate results gathered across a spectrum of studies and to generate a
249 rigorously monitored database focused on mitochondrial respiratory function. In this way,

250 researchers within the same and across different disciplines will be positioned to compare their
251 findings to an agreed upon set of clearly defined and accepted international standards.

252 Reliability and comparability of quantitative results depend on the accuracy of
253 measurements under strictly-defined conditions. A conceptually defined framework is also
254 required to warrant meaningful interpretation and comparability of experimental outcomes
255 carried out by research groups at different institutes. With an emphasis on quality of research,
256 collected data can be useful far beyond the specific question of a particular experiment.
257 Enabling meta-analytic studies is the most economic way of providing robust answers to
258 biological questions (Cooper *et al.* 2009). Vague or ambiguous jargon can lead to confusion
259 and may relegate valuable signals to wasteful noise. For this reason, measured values must be
260 expressed in standardized units for each parameter used to define mitochondrial respiratory
261 function. Standardization of nomenclature and definition of technical terms is essential to
262 improve the awareness of the intricate meaning of a divergent scientific vocabulary, for
263 documentation and integration into databases in general, and quantitative modelling in
264 particular (Beard 2005). The focus on the protonmotive force, coupling states, and fluxes
265 through metabolic pathways of aerobic energy transformation in mitochondrial preparations is
266 a first step in the attempt to generate a harmonized and conceptually-oriented nomenclature in
267 bioenergetics and mitochondrial physiology. Coupling states of intact cells and respiratory
268 control by fuel substrates and specific inhibitors of respiratory enzymes will be reviewed in
269 subsequent communications.

270

271 **2. Respiratory coupling states in mitochondrial preparations**

272 *‘Every professional group develops its own technical jargon for talking about*
273 *matters of critical concern ... People who know a word can share that idea with*
274 *other members of their group, and a shared vocabulary is part of the glue that holds*
275 *people together and allows them to create a shared culture’ (Miller 1991).*

276 **Mitochondrial preparations** are defined as either isolated mitochondria, or tissue and
277 cellular preparations in which the barrier function of the plasma membrane is disrupted. The
278 plasma membrane separates the cytosol, nucleus, and organelles (the intracellular
279 compartment) from the environment of the cell. The plasma membrane consists of a lipid
280 bilayer, embedded proteins, and attached organic molecules that collectively control the
281 selective permeability of ions, organic molecules, and particles across the cell boundary. The
282 intact plasma membrane, therefore, prevents the passage of many water-soluble mitochondrial
283 substrates, such as succinate or adenosine diphosphate (ADP), that are required for the analysis
284 of respiratory capacity at kinetically-saturating concentrations, thus limiting the scope of
285 investigations into mitochondrial respiratory function in intact cells. The cholesterol content of
286 the plasma membrane is high compared to mitochondrial membranes. Therefore, mild
287 detergents, such as digitonin and saponin, can be applied to selectively permeabilize the plasma
288 membrane by interaction with cholesterol and allow free exchange of cytosolic components
289 with ions and organic molecules of the immediate cell environment, while maintaining the
290 integrity and localization of organelles, cytoskeleton, and the nucleus. Application of optimum
291 concentrations of these mild detergents leads to the complete loss of cell viability, tested by
292 nuclear staining, while mitochondrial function remains intact, as shown by an unaltered
293 respiration rate of isolated mitochondria after the addition of such low concentrations of digitonin
294 and saponin. In addition to mechanical permeabilization during homogenization of fresh tissue,
295 saponin may be applied to ensure permeabilization of all cells. Crude homogenate and cells
296 permeabilized in the respiration chamber contain all components of the cell at highly diluted
297 concentrations. All mitochondria are retained in chemically-permeabilized mitochondrial
298 preparations and crude tissue homogenates. In the preparation of isolated mitochondria, the
299 cells or tissues are homogenized, and the mitochondria are separated from other cell fractions
300 and purified by differential centrifugation, entailing the loss of a significant fraction of

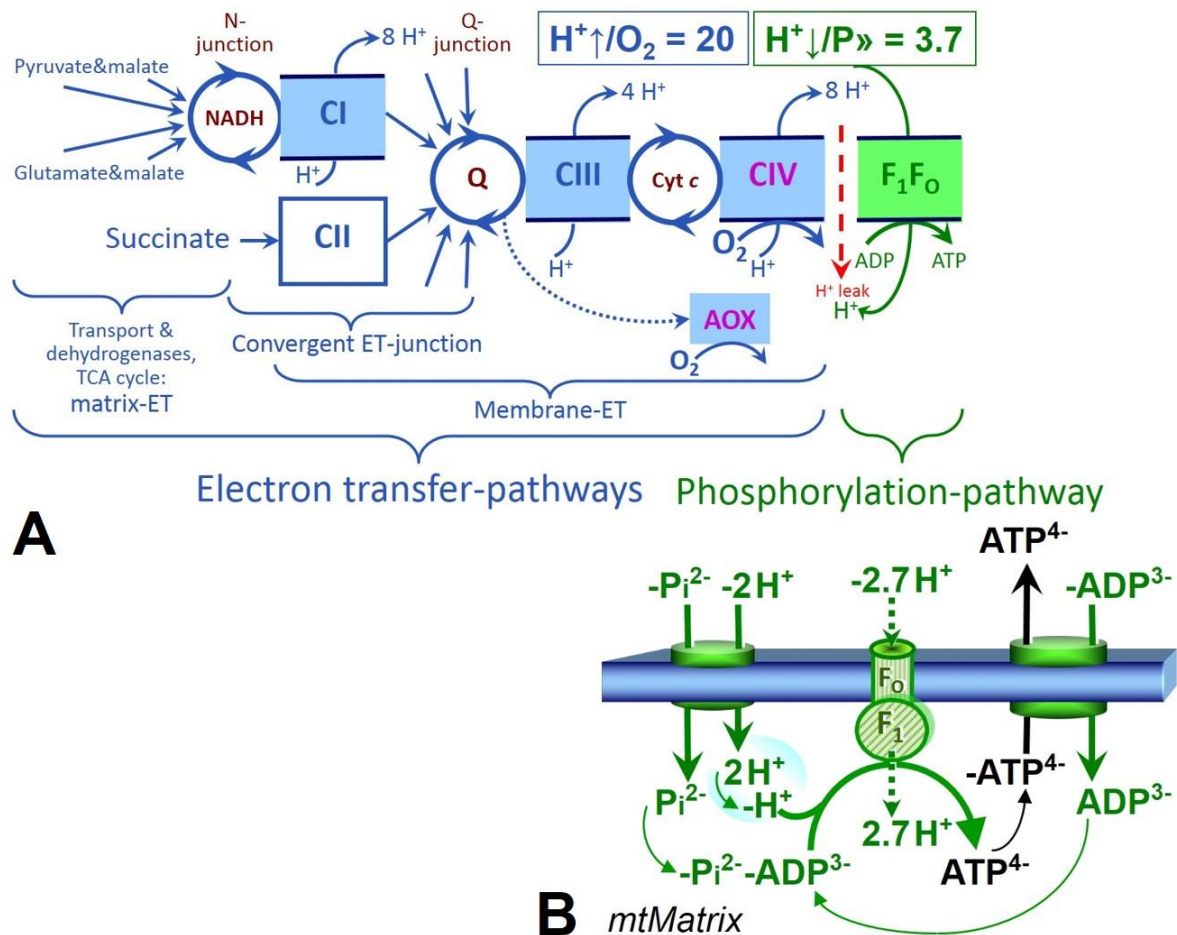
301 mitochondria. The term mitochondrial preparation does not include further fractionation of
302 mitochondrial components, as well as submitochondrial particles.

303

304 *2.1. Three coupling states of mitochondrial preparations and residual oxygen consumption*

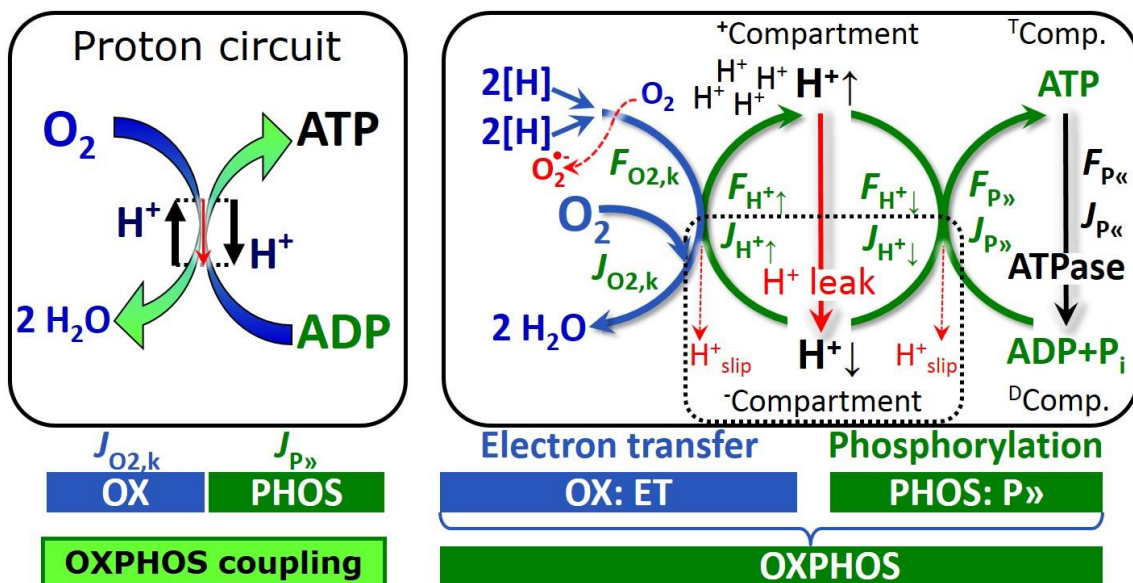
305 **Respiratory capacities in coupling control states:** To extend the classical nomenclature
306 on mitochondrial coupling states (Section 2.4) by a concept-driven terminology that
307 incorporates explicit information on the nature of the respiratory states, the terminology must
308 be general and not restricted to any particular experimental protocol or mitochondrial
309 preparation (Gnaiger 2009). We focus primarily on the conceptual ‘why’, along with
310 clarification of the experimental ‘how’. In the following section, the concept-driven
311 terminology is explained and coupling states are defined. We define respiratory capacities,
312 comparable to channel capacity in information theory (Schneider 2006), as the upper bound of
313 the rate of respiration measured in defined coupling and electron transfer-pathway (ET-
314 pathway) control states. To provide a diagnostic reference for respiratory capacities of core
315 energy metabolism, the capacity of *oxidative phosphorylation*, OXPHOS, is measured at
316 kinetically-saturating concentrations of ADP and inorganic phosphate, P_i . The *oxidative* ET-
317 capacity reveals the limitation of OXPHOS-capacity mediated by the *phosphorylation-*
318 *pathway*. The ET- and phosphorylation-pathways comprise coupled segments of the OXPHOS-
319 pathway. ET-capacity is measured as noncoupled respiration by application of *external*
320 *uncouplers*. The contribution of *intrinsically uncoupled* oxygen consumption is most easily
321 studied in the absence of ADP, *i.e.* by not stimulating phosphorylation, or by inhibition of the
322 phosphorylation-pathway. The corresponding states are collectively classified as LEAK-states,
323 when oxygen consumption compensates mainly for the proton leak (**Table 1**). Different
324 coupling states are induced by (1) adding ADP or P_i , (2) inhibiting the phosphorylation-
325 pathway, and (3) performing uncoupler titrations, while maintaining a defined ET-pathway
326 state with constant fuel substrates and ET inhibitors (**Fig. 1**).

327 **Kinetic control:** Coupling control states are established in the study of mitochondrial
 328 preparations to obtain reference values for various output variables. Physiological conditions *in*
 329 *vivo* may deviate substantially from these experimentally obtained states. Since kinetically-
 330 saturating concentrations, *e.g.* of ADP or oxygen, may not apply to physiological intracellular
 331 conditions, relevant information is obtained in studies of kinetic responses to conditions
 332 intermediate between the LEAK state at zero [ADP] and the OXPHOS-state at saturating
 333 [ADP], or of respiratory capacities in the range between kinetically-saturating [O₂] and anoxia
 334 (Gnaiger 2001).



335
 336 **Fig. 1. The oxidative phosphorylation-pathway, OXPHOS-pathway.** (A) Electron transfer, ET,
 337 coupled to phosphorylation. ET-pathways converge at the N- and Q-junction, as shown for the NADH-
 338 and succinate-pathway; additional arrows indicate electron entry to the Q-junction through electron
 339 transferring flavoprotein, glycerophosphate dehydrogenase, dihydro-oxaloacetate dehydrogenase, choline
 340 dehydrogenase, and sulfide-ubiquinone oxidoreductase. The branched pathway of oxygen consumption

341 by alternative quinol oxidase (AOX) is indicated by the dotted arrow. The $H^+ \uparrow / O_2$ ratio is the outward
 342 proton flux from the matrix space divided by catabolic O_2 flux in the NADH-pathway. The $H^+ \downarrow / P \gg$ ratio is
 343 the inward proton flux from the inter-membrane space divided by the flux of phosphorylation of ADP to
 344 ATP. Due to proton leak and slip these are not fixed stoichiometries. (B) Phosphorylation-pathway
 345 catalyzed by the F_1F_0 ATP synthase, adenine nucleotide translocase, and inorganic phosphate
 346 transporter. The $H^+ \downarrow / P \gg$ stoichiometry is the sum of the coupling stoichiometry in the ATP synthase
 347 reaction ($-2.7 H^+$ from the intermembrane space, $2.7 H^+$ to the matrix) and the proton balance in the
 348 translocation of ADP^{2-} , ATP^{3-} and P_i^{2-} . See Eqs. 3 and 4 for further explanation. Modified from (A)
 349 Lemieux *et al.* (2017) and (B) Gnaiger (2014).
 350



351
 352 **Fig. 2. The proton circuit and coupling in oxidative phosphorylation (OXPHOS).** Oxygen flux, $J_{O_2,k}$,
 353 through the catabolic ET-pathway k is coupled to flux through the phosphorylation-pathway of ADP to
 354 ATP, $J_{P \gg}$, by the proton pumps of the ET-pathway, pushing the outward proton flux, $J_{H^+ \uparrow}$, and generating
 355 the output protonmotive force, $F_{H^+ \uparrow}$. ATP synthase is coupled to inward proton flux, $J_{H^+ \downarrow}$, to phosphorylate
 356 $ADP + P_i$ to ATP, driven by the input protonmotive force, $F_{H^+ \downarrow} = -F_{H^+ \uparrow}$. $2[H]$ indicates the reduced hydrogen
 357 equivalents of fuel substrates that provide the chemical input force, $F_{O_2,k}$ [kJ/mol O_2], of the catabolic
 358 reaction k with oxygen (Gibbs energy of reaction per mole O_2 consumed in reaction k), typically in the
 359 range of -460 to -480 kJ/mol. The output force is given by the phosphorylation potential difference (ADP
 360 phosphorylated to ATP), $F_{P \gg}$, which varies *in vivo* ranging from about 48 to 62 kJ/mol under physiological
 361 conditions (Gnaiger 1993a). Fluxes, J_B , and forces, F_B , are expressed in either chemical units,

362 [mol·s⁻¹·m⁻³] and [J·mol⁻¹] respectively, or electrical units, [C·s⁻¹·m⁻³] and [J·C⁻¹] respectively. Vectorial
 363 and scalar fluxes are expressed per volume, V [m³], of the system. The system defined by the
 364 boundaries shown as a full black line is not a black box, but is analysed as a compartmental system.
 365 The negative compartment (⁻Compartment, enclosed by the dotted line) is the matrix space, separated
 366 from the positive compartment (⁺Compartment) by the mtIM. ADP+P_i and ATP are the substrate- and
 367 product-compartments (scalar ADP and ATP compartments, ^DComp. and ^TComp.), respectively.
 368 Chemical potentials of all substrates and products involved in the scalar reactions are measured in the
 369 ⁺Compartment for calculation of the scalar forces $F_{O_2,k}$ and $F_{P\gg} = -F_{P\ll}$ (**Box 2**). Modified from Gnaiger
 370 (2014).

371

372 **Phosphorylation, P \gg** : *Phosphorylation* in the context of OXPHOS is defined as
 373 phosphorylation of ADP to ATP. On the other hand, the term phosphorylation is used generally
 374 in many different contexts, *e.g.* protein phosphorylation. This justifies consideration of a
 375 symbol more discriminating and specific than P as used in the P/O ratio (phosphate to atomic
 376 oxygen ratio; $O = 0.5 O_2$), where P indicates phosphorylation of ADP to ATP or GDP to GTP.
 377 We propose the symbol P \gg for the endergonic direction of phosphorylation ADP→ATP, and
 378 likewise the symbol P \ll for the corresponding exergonic hydrolysis ATP→ADP (**Fig. 2; Box**
 379 **3**). ATP synthase is the proton pump of the phosphorylation-pathway (**Fig. 1B**). P \gg may also
 380 involve substrate-level phosphorylation as part of the tricarboxylic acid cycle (succinyl-CoA
 381 ligase) and phosphorylation of ADP catalyzed by phosphoenolpyruvate carboxykinase,
 382 adenylate kinase, creatine kinase, hexokinase and nucleoside diphosphate kinase (NDPK).
 383 Kinase cycles are involved in intracellular energy transfer and signal transduction for regulation
 384 of energy flux. In isolated mammalian mitochondria ATP production catalyzed by adenylate
 385 kinase, $2ADP \leftrightarrow ATP + AMP$, proceeds without fuel substrates in the presence of ADP
 386 (Komlódi and Tretter 2017). $J_{P\gg}/J_{O_2,k}$ (P \gg /O₂) is two times the ‘P/O’ ratio of classical
 387 bioenergetics. The effective P \gg /O₂ ratio is diminished by: (1) the proton leak across the mtIM
 388 from low pH in the ⁺Compartment to high pH in the ⁻Compartment; (2) cycling of other cations;

389 (3) proton slip in the proton pumps when a proton effectively is not pumped; and (4) electron
 390 leak in the univalent reduction of oxygen (O_2 ; dioxygen) to superoxide anion radical ($O_2^{\bullet-}$).

391

392 **Table 1. Coupling states and residual oxygen consumption in mitochondrial**
 393 **preparations in relation to respiration- and phosphorylation-rate, $J_{O_2,k}$ and $J_{P_{\gg}}$,**
 394 **and protonmotive force, $F_{H^+\uparrow}$.** Coupling states are established at kinetically-
 395 saturating concentrations of fuel substrates and O_2 .

State	$J_{O_2,k}$	$J_{P_{\gg}}$	$F_{H^+\uparrow}$	Inducing factors	Limiting factors
LEAK	L ; low proton leak-dependent respiration	0	max.	Proton leak, slip, and cation cycling	$J_{P_{\gg}} = 0$: (1) without ADP, L_N ; (2) max. ATP/ADP ratio, L_T ; or (3) inhibition of the phosphorylation-pathway, L_{Omy}
OXPHOS	P ; high ADP-stimulated respiration	max.	high	Kinetically-saturating [ADP] and $[P_i]$	$J_{P_{\gg}}$ by phosphorylation-pathway; or $J_{O_2,k}$ by ET-capacity
ET	E ; max. noncoupled respiration	0	low	Optimal external uncoupler concentration for max. oxygen flux	$J_{O_2,k}$ by ET-capacity
ROX	R_{ox} ; min. residual O_2 consumption	0	0	$J_{O_2,R_{ox}}$ in non-ET-pathway oxidation reactions	Full inhibition of ET-pathway or absence of fuel substrates

396

397

398
 399 **LEAK-state (Fig. 3):** The
 400 LEAK-state is defined as a state
 401 of mitochondrial respiration when
 402 O₂ flux mainly compensates for
 403 the proton leak in the absence of
 404 ATP synthesis, at kinetically-

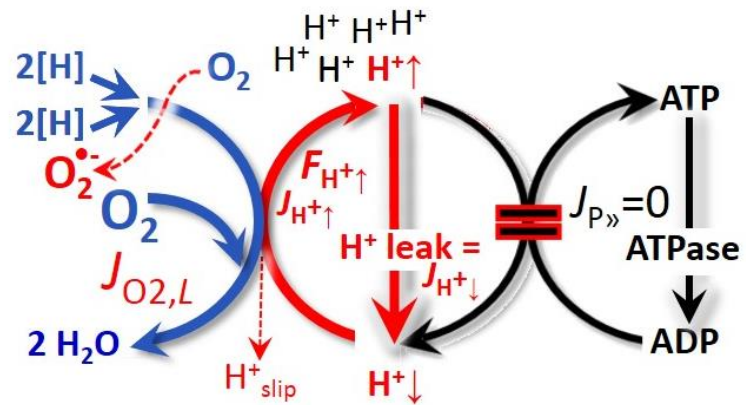


Fig. 3. LEAK-state: Phosphorylation is arrested, $J_{P} = 0$, and oxygen flux, $J_{O_2,L}$, is controlled mainly by the proton leak, which equals $J_{H^+↓}$, at maximum protonmotive force, $F_{H^+↑}$. See also Fig. 2.

405 saturating concentrations of O₂
 406 and respiratory fuel substrates.
 407 LEAK-respiration is measured to
 408 obtain an indirect estimate of
 409 *intrinsic uncoupling* without addition of any experimental uncoupler: (1) in the absence of
 410 adenylates; (2) after depletion of ADP at maximum ATP/ADP ratio; or (3) after inhibition of
 411 the phosphorylation-pathway by inhibitors of ATP synthase, such as oligomycin, or adenine
 412 nucleotide translocase, such as carboxyatractyloside.

413

414 **Table 2. Distinction of terms related to coupling.**

Term	Respiration	P _» /O ₂	Note
Fully coupled	$P - L$	max.	OXPPOS-capacity corrected for LEAK-respiration (Fig. 6)
Well-coupled	P	high	Phosphorylating respiration with an intrinsic LEAK component (Fig. 4)
Loosely coupled	up to E	low	Inducibly uncoupled by UCP1 or Ca ²⁺ cycling
Dyscoupled	P	low	Pathologically, toxicologically, environmentally increased uncoupling, mitochondrial dysfunction
Uncoupled and Decoupled	L	0	Non-phosphorylating intrinsic LEAK-respiration without added protonophore (Fig. 3)
Noncoupled	E	0	Non-phosphorylating respiration stimulated to maximum flux at optimum exogenous uncoupler concentration (Fig. 5)

415

416 **Proton leak:** Proton leak is the *uncoupled* process in which protons diffuse across the
417 mtIM in the dissipative direction of the downhill protonmotive force without coupling to
418 phosphorylation (**Fig. 3**). The proton leak flux, F_{H^+} , depends non-linearly on the protonmotive
419 force (Garlid *et al.* 1989; Divakaruni and Brand 2011), is a property of the mtIM, may be
420 enhanced due to possible contaminations by free fatty acids, and is physiologically controlled.
421 In particular, inducible uncoupling mediated by uncoupling protein 1 (UCP1) is physiologically
422 controlled, *e.g.*, in brown adipose tissue. UCP1 is a proton channel of the mtIM facilitating the
423 conductance of protons across the mtIM (Klingenberg 2017). As a consequence of this effective
424 short-circuit, the protonmotive force diminishes, resulting in stimulation of electron transfer to
425 oxygen and heat dissipation without phosphorylation of ADP. Mitochondrial injuries may lead
426 to *dyscoupling* as a pathological or toxicological cause of *uncoupled* respiration, *e.g.*, as a
427 consequence of opening the permeability transition pore. Dyscoupled respiration is
428 distinguished from the experimentally induced *noncoupled* respiration in the ET-state. Under
429 physiological conditions, the proton leak is the dominant contributor to the overall leak current
430 (Dufour *et al.* 1996).

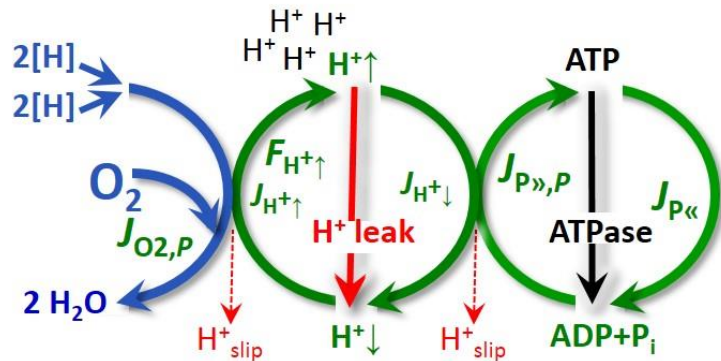
431 **Proton slip:** Proton slip is the *decoupled* process in which protons are only partially
432 translocated by a proton pump of the ET-pathways and slip back to the original compartment
433 (Dufour *et al.* 1996). Proton slip can also happen in association with the ATP-synthase, in which
434 case the proton slips downhill across the membrane to the matrix without contributing to ATP
435 synthesis. In each case, proton slip is a property of the proton pump and increases with the
436 turnover rate of the pump.

437 **Cation cycling:** Proton leak is a leak current of protons. There can be other cation
438 contributors to leak current including calcium and probably magnesium. Calcium current is
439 balanced by mitochondrial Na/Ca exchange, which is balanced by Na/H exchange or K/H
440 exchange. This is another effective uncoupling mechanism different from proton leak and slip.

441 Small differences of terms, *e.g.*, uncoupled, noncoupled, are easily overlooked and may
 442 be erroneously perceived as identical. Even with an attempt at rigorous definition, the common
 443 use of such terms may remain vague (**Table 2**).

444 **OXPHOS-state (Fig. 4):**

445 The OXPHOS-state is defined as
 446 the respiratory state with
 447 kinetically-saturating
 448 concentrations of O₂, respiratory
 449 and phosphorylation substrates,
 450 and absence of exogenous
 451 uncoupler, which provides an
 452 estimate of the maximal
 453 respiratory capacity in the



454 **Fig. 4. OXPHOS-state:** Phosphorylation, $J_{P\gg}$, is stimulated
 455 by kinetically-saturating [ADP] and inorganic phosphate,
 456 [P_i], and is supported by a high protonmotive force, $F_{H^+\uparrow}$. O₂
 457 flux, $J_{O_2,P}$, is well-coupled at a $P\gg/O_2$ ratio of $J_{P\gg,P}/J_{O_2,P}$ (See
 458 also Fig. 2).

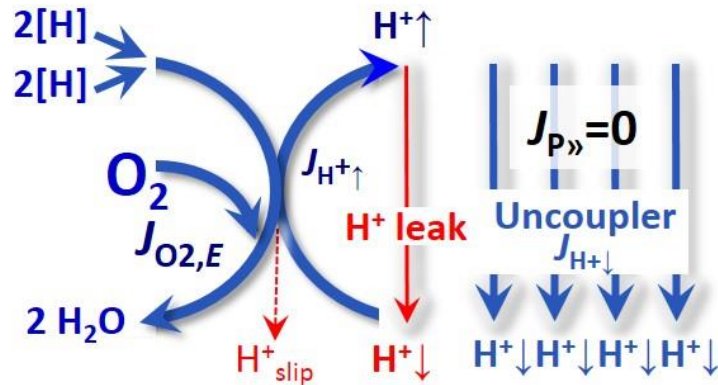
454 OXPHOS-state for any given ET-pathway state. Respiratory capacities at kinetically-saturating
 455 substrate concentrations provide reference values or upper limits of performance, aiming at the
 456 generation of data sets for comparative purposes. Physiological activities and effects of
 457 substrate kinetics can be evaluated relative to OXPHOS capacities.

458 As discussed previously, 0.2 mM ADP does not fully saturate flux in isolated
 459 mitochondria (Gnaiger 2001; Puchowicz *et al.* 2004); greater ADP concentration is required,
 460 particularly in permeabilized muscle fibres and cardiomyocytes, to overcome limitations by
 461 intracellular diffusion and by the reduced conductance of the mitochondrial outer membrane,
 462 mtOM (Jepihhina *et al.* 2011, Illaste *et al.* 2012, Simson *et al.* 2016), either through interaction
 463 with tubulin (Rostovtseva *et al.* 2008) or other intracellular structures (Birkedal *et al.* 2014). In
 464 permeabilized muscle fibre bundles of high respiratory capacity, the apparent K_m for ADP
 465 increases up to 0.5 mM (Saks *et al.* 1998), indicating that >90% saturation is reached only at
 466 >5 mM ADP. Similar ADP concentrations are also required for accurate determination of

467 OXPHOS-capacity in human clinical cancer samples and permeabilized cells (Klepinin *et al.*
 468 2016; Koit *et al.* 2017). Whereas 2.5 to 5 mM ADP is sufficient to obtain the actual OXPHOS-
 469 capacity in many types of permeabilized tissue and cell preparations, experimental validation
 470 is required in each specific case.

471 Electron transfer-state

472 (Fig. 5): The ET-state is defined
 473 as the *noncoupled* state with
 474 kinetically-saturating
 475 concentrations of O₂, respiratory
 476 substrate and optimum
 477 *exogenous* uncoupler
 478 concentration for maximum O₂
 479 flux, as an estimate of oxidative



480 **Fig. 5. ET-state:** Noncoupled respiration, $J_{O_2,E}$, is maximum
 481 at optimum exogenous uncoupler concentration and
 482 phosphorylation is zero, $J_{P} = 0$ (See also Fig. 2).

480 ET-capacity. Inhibition of respiration is observed at higher than optimum uncoupler
 481 concentrations. As a consequence of the nearly collapsed protonmotive force, the driving force
 482 is insufficient for phosphorylation and $J_{P} = 0$.

483 Besides the three fundamental coupling states of mitochondrial preparations, the
 484 following respiratory state also is relevant to assess respiratory function:

485 **ROX:** Residual oxygen consumption (ROX) is defined as O₂ consumption due to
 486 oxidative side reactions remaining after inhibition of ET with rotenone, malonic acid and
 487 antimycin A. Cyanide and azide not only inhibit CIV but several peroxidases which might be
 488 involved in ROX. ROX is not a coupling state but represents a baseline that is used to correct
 489 mitochondrial respiration in defined coupling states. ROX is not necessarily equivalent to non-
 490 mitochondrial respiration, considering oxygen-consuming reactions in mitochondria not related
 491 to ET, such as oxygen consumption in reactions catalyzed by monoamine oxidases (type A and
 492 B), monooxygenases (cytochrome P450 monooxygenases), dioxygenase (sulfur dioxygenase

493 and trimethyllysine dioxygenase), several hydroxylases, and more. Mitochondrial preparations,
 494 especially those obtained from liver, may be contaminated by peroxisomes. This fact makes the
 495 exact determination of mitochondrial oxygen consumption and mitochondria-associated
 496 generation of reactive oxygen species complicated (Schönfeld *et al.* 2009). The dependence of
 497 ROX-linked oxygen consumption needs to be studied in detail with respect to non-ET enzyme
 498 activities, availability of specific substrates, oxygen concentration, and electron leakage leading
 499 to the formation of reactive oxygen species.

500

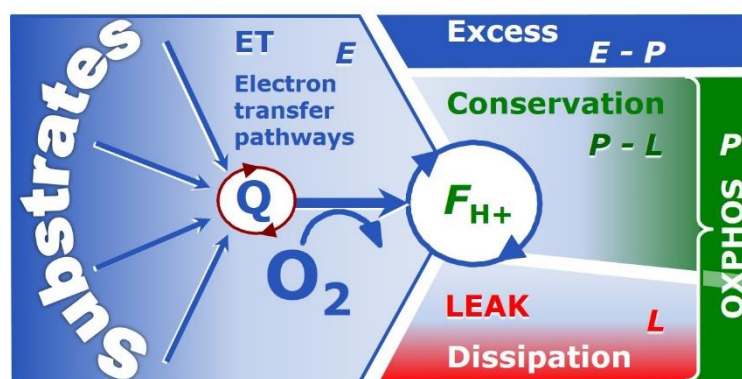
501 2.2. Coupling states and respiratory rates

502 It is important to distinguish metabolic *pathways* from metabolic *states* and the
 503 corresponding metabolic *rates*; for example: ET-pathways (**Fig. 6**), ET-state (**Fig. 5**), and ET-
 504 capacity, E , respectively (**Table 1**). The protonmotive force is *high* in the OXPHOS-state when
 505 it drives phosphorylation, *maximum* in the LEAK-state of coupled mitochondria, driven by
 506 LEAK-respiration at a minimum back flux of protons to the matrix side, and *very low* in the
 507 ET-state when uncouplers short-circuit the proton cycle (**Table 1**).

508

509 **Fig. 6. Four-compartment model**
 510 **of oxidative phosphorylation.**

511 Respiratory states (ET, OXPHOS,
 512 LEAK) and corresponding rates (E ,
 513 P , L) are connected by the
 514 protonmotive force, F_{H^+} . Electron
 515 transfer-capacity, E , is partitioned



516 into (1) dissipative LEAK-respiration, L , when the capacity to perform work is irreversibly lost, (2) net
 517 OXPHOS-capacity, $P-L$, with partial conservation of the capacity to perform work, and (3) the excess
 518 capacity, $E-P$. Modified from Gnaiger (2014).

519

520 The three coupling states, ET, LEAK and OXPHOS, are shown schematically with the
521 corresponding respiratory rates, abbreviated as E , L and P , respectively (**Fig. 6**). E may exceed
522 or be equal to P , but E cannot theoretically be lower than P . $E < P$ must be discounted as an
523 artefact, which may be caused experimentally by: (1) loss of oxidative capacity during the time
524 course of the respirometric assay, since E is measured subsequently to P ; (2) using insufficient
525 uncoupler concentrations; (3) using high uncoupler concentrations which inhibit ET (Gnaiger
526 2008); (4) high oligomycin concentrations applied for measurement of L before titrations of
527 uncoupler, when oligomycin exerts an inhibitory effect on E . On the other hand, the excess ET-
528 capacity is overestimated if non-saturating [ADP] or [P_i] are used (see State 3 in the next
529 section).

530 $E > P$ is observed in many types of mitochondria, varying between species, tissues and
531 cell types. It is the excess ET-capacity pushing the phosphorylation-flux (**Fig. 1B**) to the limit
532 of its *capacity of utilizing* the protonmotive force. Within any type of mitochondria, the
533 magnitude of $E > P$ depends on (1) the pathway control state with single or multiple electron
534 input into the Q-junction and involvement of three or fewer coupling sites determining the
535 H⁺↑/O₂ *coupling stoichiometry* (**Fig. 1A**); and (2) the *biochemical coupling efficiency* expressed
536 as $(E-L)/E$, since an increase of L causes P to increase towards the limit of E . The *excess E-P*
537 capacity, $E-P$, therefore, provides a sensitive diagnostic indicator of specific injuries of the
538 phosphorylation-pathway, under conditions when E remains constant but P declines relative to
539 controls (**Fig. 6**). Substrate cocktails supporting simultaneous convergent electron transfer to
540 the Q-junction for reconstitution of tricarboxylic acid cycle (TCA cycle) function establish
541 pathway control states with high ET-capacity, and consequently increase the sensitivity of the
542 $E-P$ assay.

543 When subtracting L from P , the dissipative LEAK component in the OXPHOS-state may
544 be overestimated. This can be avoided by measuring LEAK-respiration in a state when the
545 protonmotive force is adjusted to its slightly lower value in the OXPHOS-state, *e.g.*, by titration

546 of an ET inhibitor (Divakaruni and Brand 2011). Any turnover-dependent components of
 547 proton leak and slip, however, are underestimated under these conditions (Garlid *et al.* 1993).
 548 In general, it is inappropriate to use the term *ATP production* or *ATP turnover* for the difference
 549 of oxygen consumption measured in states *P* and *L*. The difference *P-L* is the upper limit of the
 550 part of OXPHOS-capacity that is freely available for ATP production (corrected for LEAK-
 551 respiration) and is fully coupled to phosphorylation with a maximum mechanistic stoichiometry
 552 (Fig. 6).

553

554 2.3. Classical terminology for isolated mitochondria

555 *‘When a code is familiar enough, it ceases appearing like a code; one forgets that*
 556 *there is a decoding mechanism. The message is identical with its meaning’*
 557 (Hofstadter 1979).

558 Chance and Williams (1955; 1956) introduced five classical states of mitochondrial respiration
 559 and cytochrome redox states. **Table 3** shows a protocol with isolated mitochondria in a closed
 560 respirometric chamber, defining a sequence of respiratory states.

561 **Table 3. Metabolic states of mitochondria (Chance and**
 562 **Williams, 1956; Table V).**
 563

State	[O ₂]	ADP level	Substrate level	Respiration rate	Rate-limiting substance
1	>0	low	Low	slow	ADP
2	>0	high	~0	slow	substrate
3	>0	high	High	fast	respiratory chain
4	>0	low	High	slow	ADP
5	0	high	High	0	oxygen

564

565 **State 1** is obtained after addition of isolated mitochondria to air-saturated
 566 isoosmotic/isotonic respiration medium containing inorganic phosphate, but no fuel substrates
 567 and no adenylates, *i.e.*, AMP, ADP, ATP.

568 **State 2** is induced by addition of a high concentration of ADP (typically 100 to 300 μM),
569 which stimulates respiration transiently on the basis of endogenous fuel substrates and
570 phosphorylates only a small portion of the added ADP. State 2 is then obtained at a low
571 respiratory activity limited by zero endogenous fuel substrate availability (**Table 3**). If addition
572 of specific inhibitors of respiratory complexes, such as rotenone, does not cause a further
573 decline of oxygen consumption, State 2 is equivalent to residual oxygen consumption (See
574 below). If inhibition is observed, undefined endogenous fuel substrates are a confounding factor
575 of pathway control by externally added substrates and inhibitors. In contrast to the original
576 protocol, an alternative sequence of titration steps is frequently applied, in which the alternative
577 State 2 has an entirely different meaning, when this second state is induced by addition of fuel
578 substrate without ADP (LEAK-state; in contrast to State 2 defined in **Table 2** as a ROX state),
579 followed by addition of ADP.

580 **State 3** is the state stimulated by addition of fuel substrates while the ADP concentration
581 is still high (**Table 3**) and supports coupled energy transformation through oxidative
582 phosphorylation. 'High ADP' is a concentration of ADP specifically selected to allow the
583 measurement of State 3 to State 4 transitions of isolated mitochondria in a closed respirometric
584 chamber. Repeated ADP titration re-establishes State 3 at 'high ADP'. Starting at oxygen
585 concentrations near air-saturation (ca. 200 μM O_2 at sea level and 37 $^\circ\text{C}$), the total ADP
586 concentration added must be low enough (typically 100 to 300 μM) to allow phosphorylation
587 to ATP at a coupled oxygen consumption that does not lead to oxygen depletion during the
588 transition to State 4. In contrast, kinetically-saturating ADP concentrations usually are an order
589 of magnitude higher than 'high ADP', *e.g.* 2.5 mM in isolated mitochondria. The abbreviation
590 State 3u is frequently used in bioenergetics, to indicate the state of respiration after titration of
591 an uncoupler, without sufficient emphasis on the fundamental difference between OXPHOS-
592 capacity (*well-coupled* with an *endogenous* uncoupled component) and ET-capacity
593 (*noncoupled*).

594 **State 4** is a LEAK-state that is obtained only if the mitochondrial preparation is intact
 595 and well-coupled. Depletion of ADP by phosphorylation to ATP leads to a decline in oxygen
 596 consumption in the transition from State 3 to State 4. Under these conditions, a maximum
 597 protonmotive force and high ATP/ADP ratio are maintained, and the P_{\gg}/O_2 ratio can be
 598 calculated. State 4 respiration, L_T (**Table 1**), reflects intrinsic proton leak and intrinsic ATP
 599 hydrolysis activity. Oxygen consumption in State 4 is an overestimation of LEAK-respiration
 600 if the contaminating ATP hydrolysis activity recycles some ATP to ADP, $J_{P\ll}$, which stimulates
 601 respiration coupled to phosphorylation, $J_{P\gg} > 0$. This can be tested by inhibition of the
 602 phosphorylation-pathway using oligomycin, ensuring that $J_{P\gg} = 0$ (State 4o). Alternatively,
 603 sequential ADP titrations re-establish State 3, followed by State 3 to State 4 transitions while
 604 sufficient oxygen is available. However, anoxia may be reached before exhaustion of ADP
 605 (State 5).

606 **State 5** is the state after exhaustion of oxygen in a closed respirometric chamber.
 607 Diffusion of oxygen from the surroundings into the aqueous solution may be a confounding
 608 factor preventing complete anoxia (Gnaiger 2001). Chance and Williams (1955) provide an
 609 alternative definition of State 5, which gives it the meaning of ROX: ‘State 5 may be obtained
 610 by antimycin A treatment or by anaerobiosis’.

611 In **Table 3**, only States 3 and 4 (and ‘State 2’ in the alternative protocol without ADP;
 612 not included in the table) are coupling control states, with the restriction that O_2 flux in State 3
 613 may be limited kinetically by non-saturating ADP concentrations (**Table 1**).

614

615 **3. The protonmotive force and proton flux**

616 *3.1. Electric and chemical partial forces versus electrical and chemical units*

617 The protonmotive force across the mtIM (Mitchell 1961; Mitchell and Moyle 1967) was
 618 introduced most beautifully in the *Grey Book 1966* (see Mitchell 2011),

$$619 \quad \Delta p = \Delta \Psi + \Delta \mu_{H^+}/F \quad (\text{Eq. 1})$$

620 The protonmotive force, Δp , consists of two partial forces: (1) The electrical part, $\Delta\Psi$, is the
 621 difference of charge (electric potential difference), is not specific for H^+ , and can, therefore, be
 622 measured by the distribution of other permeable cations between the positive and negative
 623 compartment (**Fig. 2**). (2) The chemical part, $\Delta\mu_{H^+}$, is the chemical potential difference in H^+ ,
 624 is proportional to the pH difference, and incorporates the Faraday constant (**Table 4**).

625
 626 **Table 4. Protonmotive force and flux matrix.** Columns: The protonmotive force is
 627 the sum of *partial isomorphic forces*, F_{el} and $F_{H^+,d}$. Rows: Electrical and chemical
 628 formats (motive units MU, C and mol, for e and n , respectively). The Faraday constant,
 629 F , converts protonmotive force and flux from format e to n . In contrast to force (state),
 630 the conjugated flux (rate) cannot be partitioned.
 631

State	Force		electric	+	chem.	Unit	Notes
Protonmotive force, e	Δp	=	$\Delta\Psi$	+	$\Delta\mu_{H^+}/F$	$J\cdot C^{-1}$	1e
Chemiosmotic potential, n	$\Delta\tilde{\mu}_{H^+}$	=	$\Delta\Psi\cdot F$	+	$\Delta\mu_{H^+}$	$J\cdot mol^{-1}$	1n
State	Isomorphic force		eI	+	H^+_d	$J\cdot MU^{-1}$	
Electric charge, e	$F_{H^+/e}$	=	$F_{el/e}$	+	$F_{H^+,d/e}$	$J\cdot C^{-1}$	2e
Amount of substance, n	$F_{H^+/n}$	=	$F_{el/n}$	+	$F_{H^+,d/n}$	$J\cdot mol^{-1}$	2n
Rate	Isomorphic flux		e	or	n	$MU\cdot s^{-1}\cdot m^{-3}$	
Electric charge, e	$J_{H^+/e}$		$J_{H^+/e}$			$C\cdot s^{-1}\cdot m^{-3}$	3e
Amount of substance, n	$J_{H^+/n}$				$J_{H^+/n}$	$mol\cdot s^{-1}\cdot m^{-3}$	3n

632
 633 1: The Faraday constant, F , is the product of elementary charge ($e = 1.602177\cdot 10^{-19}\cdot C$) and the
 634 Avogadro (Loschmidt) constant ($L = 6.022136\cdot 10^{23}\cdot mol^{-1}$), $F = eF = 96,485.3 C\cdot mol^{-1}$, *i.e.* the
 635 conversion factor between electrical and chemical units. $\Delta\tilde{\mu}_{H^+}$ is the chemiosmotic potential
 636 difference. 1e and 1n are the classical representations of 2e and 2n.

637 2: F_{H^+} is the protonmotive force expressed in formats e or n , expressed in units C or mol. $F_{el/e} \equiv \Delta\Psi$ is
 638 the partial protonmotive force (eI) acting generally on charged motive molecules (*i.e.* ions that are
 639 permeable across the mtIM). In contrast, $F_{H^+,d/n} \equiv \Delta\mu_{H^+}$ is the partial protonmotive force specific for
 640 proton diffusion, H^+_d . The sign of the force is negative for exergonic transformations in which exergy

641 is lost or dissipated, $F_{H+\downarrow}$, and positive for endergonic transformations which conserve exergy in a
 642 coupled exergonic process, $F_{H+\uparrow} = -F_{H+\downarrow}$ (**Box 3**).

643 3: The sign of the flux, J_{H+} , depends on the definition of the compartmental direction of the translocation.
 644 For the outward direction, $J_{H+\uparrow}$, flux is positive since the direction involves formation of H^+ in the
 645 $^+$ Compartment ($H^+\uparrow$ is added, $v_{H+\uparrow} = 1$; and $H^+\downarrow$ is removed, $v_{H+\downarrow} = -1$). Equally, $J_{H+\downarrow}$ is positive since
 646 the direction involves formation of H^+ in the $^-$ Compartment ($H^+\downarrow$ is added, $v_{H+\downarrow} = 1$; and $H^+\uparrow$ is
 647 removed, $v_{H+\uparrow} = -1$; **Fig. 2**). The product of flux and force is volume-specific power [$J \cdot s^{-1} \cdot m^{-3} = W \cdot m^{-3}$]:
 648 $P_{V,H+} = J_{H+\uparrow/e} \cdot F_{H+\uparrow/e} = J_{H+\uparrow/n} \cdot F_{H+\uparrow/n}$.

650 **Faraday constant**, $F = eL$ [C/mol] (**Table 4**, note 1) enables the conversion between
 651 protonmotive force, $F_{H+/e} \equiv \Delta p$ [J/C], expressed per *motive charge*, e [C], and protonmotive
 652 force or electrochemical potential difference, $F_{H+/n} \equiv \Delta \tilde{\mu}_{H+} = \Delta p \cdot F$ [J/mol], expressed per
 653 *motive amount of protons*, n [mol]. Proton charge, e , and amount of substance, n , are motive
 654 entities expressed in units C and mol, respectively. Taken together, F is the conversion factor
 655 for expressing protonmotive force and flux in motive units of e or n (Eq. 2; **Table 4**, Notes 1
 656 and 2),

$$657 \quad F_{H+/n} = F_{H+/e} \cdot eL \quad (\text{Eq. 2.1})$$

$$658 \quad J_{H+/n} = J_{H+/e} / (eL) \quad (\text{Eq. 2.2})$$

659 In each format, the protonmotive force is expressed as the sum of two partial isomorphic
 660 forces. The complex symbols in Eq. 1 can be explained and visualized more explicitly by
 661 *partial isomorphic forces* as the components of the protonmotive force:

662 **Electric part of the protonmotive force:** (1) Isomorph e : $F_{el/e} \equiv \Delta \Psi$ is the electric part
 663 of the protonmotive force expressed in electrical units joule per coulomb, *i.e.* volt [$V = J/C$].
 664 $F_{el/e}$ is defined as partial Gibbs energy change per *motive elementary charge*, e [C], not specific
 665 for proton charge (**Table 4**, Note 2e). (2) Isomorph n : $F_{el/n} \equiv \Delta \Psi \cdot F$ is the electric force expressed
 666 in chemical units joule per mole [J/mol], defined as partial Gibbs energy change per *motive*
 667 *amount of charge*, n [mol], not specific for proton charge (**Table 4**, Note 2n).

668

669 **Table 5. Power, exergy, force, flux, and advancement.**

670

Expression	Symbol	Definition	Unit	Notes
Power, volume-specific	$P_{V,tr}$	$P_{V,tr} = J_{tr} \cdot F_{tr} = d_{tr}G \cdot dt^{-1}$	$W \cdot m^{-3} =$ $J \cdot s^{-1} \cdot m^{-3}$	1
Force, isomorphic	F_{tr}	$F_{tr} = \partial G \cdot \partial_{tr}\xi^{-1}$	$J \cdot MU^{-1}$	2
Flux, isomorphic	J_{tr}	$J_{tr} = d_{tr}\xi \cdot dt^{-1} \cdot V^{-1}$	$MU \cdot s^{-1} \cdot m^{-3}$	3
Advancement, n	$d_{tr}\xi_{H+/n}$	$d_{tr}\xi_{H+/n} = d_{tr}n_{H+} \cdot \nu_{H+}^{-1}$	$MU = mol$	$4n$
Advancement, e	$d_{tr}\xi_{H+/e}$	$d_{tr}\xi_{H+/e} = d_{tr}e_{H+} \cdot \nu_{H+}^{-1}$	$MU = C$	$4e$
Electric partial force, e	$F_{el/e}$	$F_{el/e} \equiv \Delta\Psi =$ $-RT/(zF) \cdot \Delta \ln a_B$	$V = J \cdot C^{-1}$	$5e$
Electric partial force, n	$F_{el/n}$	$F_{el/n} \equiv \Delta\Psi \cdot zF = 96.5 \cdot \Delta\Psi$	$kJ \cdot mol^{-1}$	$5n$
Chemical partial force, e	$F_{H+,d/e}$	$F_{H+,d/e} \equiv \Delta\mu_{H+}/F =$ $-RT/F \cdot \ln(10) \cdot \Delta pH$ $= -0.061 \cdot \Delta pH$	$J \cdot C^{-1}$	$6e$
at 37 °C			$J \cdot C^{-1}$	
Chemical partial force, n	$F_{H+,d/n}$	$F_{H+,d/n} \equiv \Delta\mu_{H+} =$ $-RT \cdot \ln(10) \cdot \Delta pH$ $= -5.9 \cdot \Delta pH$	$J \cdot mol^{-1}$	$6n$
at 37 °C			$kJ \cdot mol^{-1}$	

671

672 1 to 4: A motive entity, expressed in a motive unit [MU] is a characteristic for any type of transformation,

673

tr. MU = mol or C in the chemical or electrical format of proton translocation.

674

2: Isomorphic forces, F_{tr} , are related to the generalized forces, X_{tr} , of irreversible thermodynamics

675

as $F_{tr} = -X_{tr} \cdot T$, and the force of chemical reactions is the negative affinity, $F_r = -A$ (Prigogine 1967).

676

 ∂G [J] is the partial Gibbs energy change in the advancement of transformation tr.

677

3: For MU = C, flow is electric current, I_{el} [$A = C \cdot s^{-1}$], vector flux is electric current density per area,

678

 J_{el} , and compartmental flux is electric current density per volume, I_{el} [$A \cdot m^{-3}$], all expressed in

679

electrical format.

680

 $4n$: For a chemical reaction, the advancement of reaction r is $d_r\xi_B = d_r n_B \cdot \nu_B^{-1}$ [mol]. The stoichiometric

681

number is $\nu_B = -1$ or $\nu_B = 1$, depending on B being a product or substrate, respectively, in reaction

682

r involving one mole of B. The conjugated *intensive* molar quantity, $F_{B,r} = \partial G / \partial_r \xi_B$ [$J \cdot mol^{-1}$], is the

683

chemical force of reaction or *reaction-motive* force per stoichiometric amount of B. In reaction

684

kinetics, $d_r n_B$ is expressed as a volume-specific quantity, which is the partial contribution to the

685

total concentration change of B, $d_r c_B = d_r n_B / V$ and $d_e c_B = d_e n_B / V$, respectively. In open systems with

686

constant volume V , $d_c c_B = d_r c_B + d_e c_B$, where r indicates the *internal* reaction and e indicates the

687 external flux of B into the unit volume of the system. At steady state the concentration does not
 688 change, $d_{cB} = 0$, when $d_{r,cB}$ is compensated for by the external flux of B, $d_{r,cB} = -d_e c_B$ (Gnaiger
 689 1993b). Alternatively, $d_{cB} = 0$ when B is held constant by different coupled reactions in which B
 690 acts as a substrate or a product.

691 4e: Scalar potential difference across the mitochondrial membrane. In a scalar electric transformation
 692 (flux of charge, *i.e.* volume-specific current, from the matrix space to the intermembrane and
 693 extramitochondrial space) the motive force is the difference of charge (**Box 2**). The endergonic
 694 direction of translocation is defined in **Fig. 2** as $H^+_{\downarrow} \rightarrow H^+_{\uparrow}$.

695 5e: $F = 96.5 \text{ (kJ}\cdot\text{mol}^{-1})/\text{V}$. z_B is the charge number of ion B. a_B is the (relative) activity of ion B, which
 696 in dilute solutions ($c < 0.1 \text{ mol}\cdot\text{dm}^{-3}$) is approximately equal to c_B/c° , where c° is the standard
 697 concentration of $1 \text{ mol}\cdot\text{dm}^{-3}$. $\Delta \ln a_B = \ln a_2 - \ln a_1 = \ln(a_2/a_1)$, when ion B diffuses or is translocated
 698 from compartment 1 to 2. Compartments 1 and 2 have to be defined in each case (**Fig. 2**). Note
 699 that ion selective electrodes (pH or TPP^+ electrodes) respond to $\ln a_B$. $\Delta \ln a_{H^+} = -\ln(10) \cdot \Delta \text{pH}$.

700 6: $R = 8.31451 \text{ J}\cdot\text{K}^{-1}\cdot\text{mol}^{-1}$ is the gas constant. The electric partial force is independent of
 701 temperature (Note 5), but the chemical partial force depends on absolute temperature, $T [\text{K}]$. RT
 702 = 2.479 and 2.579 $\text{kJ}\cdot\text{mol}^{-1}$ at 298.15 and 310.15 K (25 and 37 °C), respectively.

703 6e: $RT/F \cdot \Delta \ln a_{H^+}$ yields force in the electrical format [$\text{J}\cdot\text{C}^{-1} = \text{V}$]. $RT/F = 2.479$ and 2.579 mV at 298.15
 704 and 310.15 K, respectively, and $\ln(10) \cdot RT/F = 59.16$ and 61.54 mV, respectively.

705 6n: $RT \cdot \Delta \ln a_{H^+}$ yields force in the chemical format [$\text{J}\cdot\text{mol}^{-1}$]. $\ln(10) \cdot RT = 5.708$ and 5.938 $\text{kJ}\cdot\text{mol}^{-1}$ at
 706 298.15 and 310.15 K, respectively.

707

708 **Chemical part of the protonmotive force:** (1) Isomorph n : $F_{H^+,d/n} \equiv \Delta \mu_{H^+}$ is the chemical
 709 part (diffusion, displacement of H^+) of the protonmotive force expressed in units joule per mole
 710 [J/mol]. $F_{H^+,d/n}$ is defined as partial Gibbs energy change per *motive amount of protons*, n [mol]
 711 (**Table 4**, Note 2n). (2) Isomorph e : $F_{H^+,d/e} \equiv \Delta \mu_{H^+}/F$ is the chemical force expressed in units
 712 joule per coulomb [V], defined as partial Gibbs energy change per *motive amount of protons*
 713 *expressed in units of electric charge*, e [C], but specific for proton charge (**Table 4**, Note 2e).

714 Protonmotive means that there is a potential for the movement of protons, and force is a
 715 measure of the potential for motion. Motion is relative and not absolute (Principle of Galilean

716 Relativity); likewise there is no absolute potential, but (isomorphic) forces are potential
717 differences. An electric partial force expressed in the format of electric charge, $F_{\text{el}\uparrow/e}$, of 0.2 V
718 (**Table 5**, Note 5e) can be expressed equivalently in the format of amount, $F_{\text{el}\uparrow/n}$, of $19 \text{ kJ}\cdot\text{mol}^{-1}$
719 $\text{H}^+\uparrow$ (Note 5n). For a ΔpH of 1 unit, the chemical partial force in the format of amount, $F_{\text{H}^+\uparrow,d/n}$,
720 changes by $5.9 \text{ kJ}\cdot\text{mol}^{-1}$ (**Table 5**, Note 6n) and chemical force in the format of charge $F_{\text{H}^+\uparrow,d/e}$
721 changes by 0.06 V (Note 6e). Considering a driving force of $-470 \text{ kJ}\cdot\text{mol}^{-1} \text{ O}_2$ for oxidation, the
722 thermodynamic limit of the $\text{H}^+\uparrow/\text{O}_2$ ratio is reached at a value of $470/19 = 24$, compared to a
723 mechanistic stoichiometry of 20 (**Fig. 1**).

724

725 3.2. Definitions

726 **Control and regulation:** The terms metabolic *control* and *regulation* are frequently used
727 synonymously, but are distinguished in metabolic control analysis: ‘We could understand the
728 regulation as the mechanism that occurs when a system maintains some variable constant over
729 time, in spite of fluctuations in external conditions (homeostasis of the internal state). On the
730 other hand, metabolic control is the power to change the state of the metabolism in response to
731 an external signal’ (Fell 1997). Respiratory control may be induced by experimental control
732 signals that *exert* an influence on: (1) ATP demand and ADP phosphorylation-rate; (2) fuel
733 substrate composition, pathway competition; (3) available amounts of substrates and oxygen,
734 *e.g.*, starvation and hypoxia; (3) the protonmotive force, redox states, flux-force relationships,
735 coupling and efficiency; (4) Ca^{2+} and other ions including H^+ ; (5) inhibitors, *e.g.*, nitric oxide
736 or intermediary metabolites, such as oxaloacetate; (6) signalling pathways and regulatory
737 proteins, *e.g.* insulin resistance, transcription factor HIF-1 or inhibitory factor 1. *Mechanisms*
738 of respiratory control and regulation include adjustments of (1) enzyme activities by allosteric
739 mechanisms and phosphorylation, (2) enzyme content, concentrations of cofactors and
740 conserved moieties (such as adenylates, nicotinamide adenine dinucleotide [NAD^+/NADH],
741 coenzyme Q, cytochrome *c*); (3) metabolic channeling by supercomplexes; and (4)

742 mitochondrial density (enzyme concentrations and membrane area) and morphology (cristae
743 folding, fission and fusion). (5) Mitochondria are targeted directly by hormones, thereby
744 affecting their energy metabolism (Lee *et al.* 2013; Gerö and Szabo 2016; Price and Dai 2016;
745 Moreno *et al.* 2017). Evolutionary or acquired differences in the genetic and epigenetic basis
746 of mitochondrial function (or dysfunction) between subjects and gene therapy; age; gender,
747 biological sex, and hormone concentrations; life style including exercise and nutrition; and
748 environmental issues including thermal, atmospheric, toxicological and pharmacological
749 factors, exert an influence on all control mechanisms listed above (for reviews, see Brown 1992;
750 Gnaiger 1993a, 2009; 2014; Paradies *et al.* 2014; Morrow *et al.* 2017).

751 **Respiratory control and response:** Lack of control by a metabolic pathway, *e.g.*
752 phosphorylation-pathway, does mean that there will be no response to a variable activating it,
753 *e.g.* [ADP]. However, the reverse is not true as the absence of a response to [ADP] does not
754 exclude the phosphorylation-pathway from having some degree of control. The degree of
755 control of a component of the OXPHOS-pathway on an output variable, such as oxygen flux,
756 will in general be different from the degree of control on other outputs, such as phosphorylation-
757 flux or proton leak flux (**Box 2**). As such, it is necessary to be specific as to which input and
758 output are under consideration (Fell 1997). Therefore, the term respiratory control is elaborated
759 in more detail in the following section.

760 **Respiratory coupling control:** Respiratory control refers to the ability of mitochondria
761 to adjust oxygen consumption in response to external control signals by engaging various
762 mechanisms of control and regulation. Respiratory control is monitored in a mitochondrial
763 preparation under conditions defined as respiratory states. When phosphorylation of ADP to
764 ATP is stimulated or depressed, an increase or decrease is observed in electron flux linked to
765 oxygen consumption in respiratory coupling states of intact mitochondria ('controlled states' in
766 the classical terminology of bioenergetics). Alternatively, coupling of electron transfer with
767 phosphorylation is disengaged by disruption of the integrity of the mtIM or by uncouplers,

768 functioning like a clutch in a mechanical system. The corresponding coupling control state is
 769 characterized by high levels of oxygen consumption without control by phosphorylation
 770 ('uncontrolled state'). Energetic coupling is defined in **Box 4**. Loss of coupling lowers the
 771 efficiency by intrinsic uncoupling and decoupling, or pathological dyscoupling. Such
 772 generalized uncoupling is different from switching to mitochondrial pathways that involve
 773 fewer than three proton pumps ('coupling sites': Complexes CI, CIII and CIV), bypassing CI
 774 through multiple electron entries into the Q-junction (**Fig. 1**). A bypass of CIII and CIV is
 775 provided by alternative oxidases, which reduce oxygen without proton translocation.
 776 Reprogramming of mitochondrial pathways may be considered as a switch of gears (changing
 777 the stoichiometry) rather than uncoupling (loosening the stoichiometry).

778 **Pathway control states** are obtained in mitochondrial preparations by depletion of
 779 endogenous substrates and addition to the mitochondrial respiration medium of fuel substrates
 780 (CHNO) and specific inhibitors, activating selected mitochondrial pathways (**Fig. 1**). Coupling
 781 control states and pathway control states are complementary, since mitochondrial preparations
 782 depend on an exogenous supply of pathway-specific fuel substrates and oxygen (Gnaiger 2014).

783

784 **Box 2: Metabolic fluxes and flows: vectorial and scalar**

785 In mitochondrial electron transfer (**Fig. 1**), vectorial transmembrane proton flux is coupled
 786 through the proton pumps CI, CIII and CIV to the catabolic flux of scalar reactions, collectively
 787 measured as oxygen flux. In **Fig. 2**, the scalar catabolic reaction, k , of oxygen consumption,
 788 $J_{O_2,k}$ [$\text{mol}\cdot\text{s}^{-1}\cdot\text{m}^{-3}$], is expressed as oxygen flux per volume, V [m^3], of the instrumental chamber
 789 (the system).

790 Fluxes are *vectors*, if they have *spatial* direction in addition to magnitude. A vector flux
 791 (surface-density of flow) is expressed per unit cross-sectional area, A [m^2], perpendicular to the
 792 direction of flux. If *flows*, I , are defined as extensive quantities of the *system*, as vector or scalar
 793 flow, I or I [$\text{mol}\cdot\text{s}^{-1}$], respectively, then the corresponding vector and scalar *fluxes*, J , are

794 obtained as $\mathbf{J} = \mathbf{I} \cdot \mathbf{A}^{-1}$ [$\text{mol} \cdot \text{s}^{-1} \cdot \text{m}^{-2}$] and $J = I \cdot V^{-1}$ [$\text{mol} \cdot \text{s}^{-1} \cdot \text{m}^{-3}$], respectively, expressing flux as an
 795 area-specific vector or volume-specific scalar quantity.

796 Vectorial transmembrane proton fluxes, $J_{\text{H}^+\uparrow}$ and $J_{\text{H}^+\downarrow}$, are analyzed in a heterogenous
 797 compartmental system as a quantity with *directional* but not *spatial* information. Translocation
 798 of protons across the mtIM has a defined direction, either from the negative compartment
 799 (matrix space; negative or $\bar{\text{C}}$ Compartment) to the positive compartment (inter-membrane space;
 800 positive or C Compartment) or *vice versa* (**Fig. 2**). The arrows defining the direction of the
 801 translocation between the two compartments may point upwards or downwards, right or left,
 802 without any implication that these are actual directions in space. The C Compartment is neither
 803 above nor below the $\bar{\text{C}}$ Compartment in a spatial sense, but can be visualized arbitrarily in a figure
 804 in the upper position (**Fig. 2**). In general, the *compartmental direction* of vectorial translocation
 805 from the $\bar{\text{C}}$ Compartment to the C Compartment is defined by assigning the initial and final state
 806 as *ergodynamic compartments*, $\text{H}^+\downarrow \rightarrow \text{H}^+\uparrow$ or $0 = -\text{H}^+\downarrow + \text{H}^+\uparrow$, related to work (erg = work) that
 807 must be performed to lift the proton from a lower to a higher electrochemical potential or from
 808 the lower to the higher ergodynamic compartment (Gnaiger 1993b).

809 In direct analogy to *vectorial* translocation, the direction of a *scalar* chemical reaction, A
 810 $\rightarrow \text{B}$ or $0 = -\text{A} + \text{B}$, is defined by assigning substrates and products, A and B, as ergodynamic
 811 compartments. O_2 is defined as a substrate in respiratory O_2 consumption, which together with
 812 the fuel substrates comprises the substrate compartment of the catabolic reaction (**Fig. 2**).
 813 Volume-specific scalar O_2 flux is coupled (**Box 4**) to vectorial translocation. In order to
 814 establish a quantitative relation between the coupled fluxes, both $J_{\text{O}_2, \text{k}}$ and $J_{\text{H}^+\uparrow}$ must be
 815 expressed in identical units, [$\text{mol} \cdot \text{s}^{-1} \cdot \text{m}^{-3}$] or [$\text{C} \cdot \text{s}^{-1} \cdot \text{m}^{-3}$], yielding the $\text{H}^+\uparrow/\text{O}_2$ ratio (**Fig. 1**). The
 816 *vectorial* proton flux in compartmental translocation has *compartmental direction*,
 817 distinguished from a *vector* flux with *spatial direction*. Likewise, the corresponding
 818 protonmotive force is defined as an electrochemical potential *difference* between two

819 compartments, in contrast to a *gradient* across the membrane or a vector force with defined
820 spatial direction.

821

822 **The steady-state:** Mitochondria represent a thermodynamically open system functioning
823 as a biochemical transformation system in non-equilibrium states. State variables (protonmotive
824 force; redox states) and metabolic fluxes (*rates*) are measured in defined mitochondrial
825 respiratory *states*. Strictly, steady states can be obtained only in open systems, in which changes
826 due to *internal* transformations, *e.g.*, O₂ consumption, are instantaneously compensated for by
827 *external* fluxes *e.g.*, O₂ supply, such that oxygen concentration does not change in the system
828 (Gnaiger 1993b). Mitochondrial respiratory states monitored in closed systems satisfy the
829 criteria of pseudo-steady states for limited periods of time, when changes in the system
830 (concentrations of O₂, fuel substrates, ADP, P_i, H⁺) do not exert significant effects on metabolic
831 fluxes (respiration, phosphorylation). Such pseudo-steady states require respiratory media with
832 sufficient buffering capacity and kinetically-saturating concentrations of substrates to be
833 maintained, and thus depend on the kinetics of the processes under investigation. Proton
834 turnover, $J_{\infty H^+}$, and ATP turnover, $J_{\infty P}$, proceed in the steady-state at constant $F_{H^+\uparrow}$, when $J_{H^+\infty}$
835 $= J_{H^+\uparrow} = J_{H^+\downarrow}$, and at constant $F_{P\gg}$, when $J_{P\infty} = J_{P\gg} = J_{P\ll}$ (**Fig. 2**).

836

837 **Box 3: Endergonic and exergonic transformations, exergy and dissipation**

838 A chemical reaction, or any transformation, is exergonic if the Gibbs energy change (exergy)
839 of the reaction is negative at constant temperature and pressure. The sum of Gibbs energy
840 changes of all internal transformations in a system can only be negative, *i.e.* exergy is
841 irreversibly dissipated. Endergonic reactions are characterized by positive Gibbs energies of
842 reaction and cannot proceed spontaneously in the forward direction as defined. For instance,
843 the endergonic reaction P \gg is coupled to exergonic catabolic reactions, such that the total Gibbs
844 energy change is negative, *i.e.* exergy must be dissipated for the reaction to proceed (**Fig. 2**).

845 In contrast, energy cannot be lost or produced in any internal process, which is the key
846 message of the first law of thermodynamics. Thus mitochondria are the sites of energy
847 transformation but not energy production. Open and closed systems can gain energy and exergy
848 only by external fluxes, *i.e.* uptake from the environment. Exergy is the potential to perform
849 work. In the framework of flux-force relationships (**Box 4**), the *partial* derivative of Gibbs
850 energy per advancement of a transformation is an isomorphic force, F_{tr} (**Table 5**, Note 2). In
851 other words, force is equal to exergy per motive entity (in integral form, this definition takes
852 care of non-isothermal processes). This formal generalization represents an appreciation of the
853 conceptual beauty of Peter Mitchell's innovation of the protonmotive force against the
854 background of the established paradigm of the electromotive force (emf) defined at the limit of
855 zero current (Cohen *et al.* 2008).

856

857 3.3. Forces and fluxes in physics and irreversible thermodynamics

858 According to its definition in physics, a potential difference and as such the
859 *protonmotive force*, Δp , is not a force *per se* (Cohen *et al.* 2008). The fundamental forces of
860 physics are distinguished from *motive forces* of statistical and irreversible thermodynamics.
861 Complementary to the attempt towards unification of fundamental forces defined in physics,
862 the concepts of Nobel laureates Lars Onsager, Erwin Schrödinger, Ilya Prigogine and Peter
863 Mitchell (even if expressed in apparently unrelated terms) unite the diversity of *generalized* or
864 'isomorphic' *flux-force* relationships, the product of which links to entropy production and the
865 Second Law of thermodynamics (Schrödinger 1944; Prigogine 1967). A *motive force* is the
866 derivative of potentially available or 'free' energy (exergy) per *motive entity* (**Box 3**). Perhaps
867 the first account of a *motive force* in energy transformation can be traced back to the Peripatetic
868 school around 300 BC in the context of moving a lever, up to Newton's motive force
869 proportional to the alteration of motion (Coopersmith 2010). As a generalization, isomorphic
870 motive forces are considered as *entropic forces* in physics (Wang 2010).

871 **Vectorial and scalar forces, and fluxes:** In chemical reactions and osmotic or diffusion
872 processes occurring in a closed heterogeneous system, such as a chamber containing isolated
873 mitochondria, scalar transformations occur without measured spatial direction but between
874 separate compartments (translocation between the matrix and intermembrane space) or between
875 energetically-separated chemical substances (reactions from substrates to products). Hence, the
876 corresponding fluxes are not vectorial but scalar, and are expressed per volume and not per
877 membrane area (**Box 2**). The corresponding motive forces are also scalar potential *differences*
878 across the membrane (**Table 5**), without taking into account the *gradients* across the 6 nm thick
879 mtIM (Rich 2003).

880 **Coupling:** In energetics (ergodynamics), coupling is defined as an energy transformation
881 fuelled by an exergonic (downhill) input process driving the advancement of an endergonic
882 (uphill) output process. The (negative) output/input power ratio is the efficiency of a coupled
883 energy transformation (**Box 4**). At the limit of maximum efficiency of a completely coupled
884 system, the (negative) input power equals the (positive) output power, such that the total power
885 approaches zero at the maximum efficiency of 1, and the process becomes fully reversible
886 without any dissipation of exergy, *i.e.* without entropy production.

887

888 **Box 4: Coupling, power and efficiency, at constant temperature and pressure**

889 Energetic coupling means that two processes of energy transformation are linked such that the
890 input power, P_{in} , is the driving element of the output power, P_{out} , and the out/input power ratio
891 is the efficiency. In general, power is work per unit time [$J \cdot s^{-1} = W$]. When describing a system
892 with volume V without information on the internal structure, the output is defined as the *external*
893 work (exergy) performed by the *total* system on its environment. Such a system may be open
894 for any type of exchange, or closed and thus allowing only heat and work to be exchanged
895 across the system boundaries. This is the classical black box approach of thermodynamics. In
896 contrast, in a colourful compartmental analysis of *internal* energy transformations (**Fig. 2**), the

897 system is structured and described by definition of ergodynamic compartments (with
 898 information on the heterogeneity of the system; **Box 2**) and analysis of separate parts, *i.e.* a
 899 sequence of *partial* energy transformations, tr. At constant temperature and pressure, power per
 900 unit volume, $P_{V,tr} = P_{tr}/V [\text{W}\cdot\text{m}^{-3}]$, is the product of a volume-specific flux, J_{tr} , and its conjugated
 901 force, F_{tr} , and is directly linked to entropy production, $d_iS/dt = \Sigma_{tr}P_{tr}/T [\text{W}\cdot\text{K}^{-1}]$, as generalized
 902 by irreversible thermodynamics (Prigogine 1967; Gnaiger 1993a,b). Output power of proton
 903 translocation and catabolic input power are (**Fig. 2**),

904 Output:
$$P_{H^+\uparrow}/V = J_{H^+\uparrow} \cdot F_{H^+\uparrow}$$

905 Input:
$$P_k/V = J_{O_2,k} \cdot F_{O_2,k}$$

906 $F_{O_2,k}$ is the exergonic input force with a negative sign, and, $F_{H^+\uparrow}$, is the endergonic output force
 907 with a positive sign (**Box 3**). Ergodynamic efficiency is the ratio of output/input power, or the
 908 flux ratio times force ratio (Gnaiger 1993a,b),

909
$$\varepsilon = \frac{P_{H^+\uparrow}}{-P_k} = \frac{J_{H^+\uparrow}}{J_{O_2,k}} \cdot \frac{F_{H^+\uparrow}}{-F_{O_2,k}}$$

910 The concept of incomplete coupling relates exclusively to the first term, *i.e.* the flux ratio, or
 911 $H^+\uparrow/O_2$ ratio (**Fig. 1**). Likewise, respirometric definitions of the P_{\gg}/O_2 ratio and biochemical
 912 coupling efficiency (Section 3.2) consider flux ratios. In a completely coupled process, the
 913 power efficiency, ε , depends entirely on the force ratio, ranging from zero efficiency at an
 914 output force of zero, to the limiting output force and maximum efficiency of 1.0, when the total
 915 power of the coupled process, $P_t = P_k + P_{H^+\uparrow}$, equals zero, and any net flows are zero at
 916 ergodynamic equilibrium of a coupled process. Thermodynamic equilibrium is defined as the
 917 state when all potentials (all forces) are dissipated and equilibrate towards their minima of zero.
 918 In a fully or completely coupled process, output and input fluxes are directly proportional in a
 919 fixed ratio technically defined as a stoichiometric relationship (a gear ratio in a mechanical
 920 system). Such maximal stoichiometric output/input flux ratios are considered in OXPHOS
 921 analysis as the upper limits or mechanistic $H^+\uparrow/O_2$ and P_{\gg}/O_2 ratios (**Fig. 1**).

922

923 **Coupled versus bound processes:** Since the chemiosmotic theory describes the
 924 mechanisms of coupling in OXPHOS, it may be interesting to ask if the electrical and chemical
 925 parts of proton translocation are coupled processes. This is not the case according to the
 926 definition of coupling. If the coupling mechanism is disengaged, the output process becomes
 927 independent of the input process, and both proceed in their downhill (exergonic) direction (**Fig.**
 928 **2**). It is not possible to physically uncouple the electrical and chemical processes, which are
 929 only *theoretically* partitioned as electrical and chemical components. The electrical and
 930 chemical partial protonmotive *forces*, $F_{\text{el}\uparrow}$ and $F_{\text{H}\uparrow,\text{d}}$, can be measured separately. In contrast,
 931 the corresponding proton *flux*, $J_{\text{H}\uparrow}$, is non-separable, *i.e.*, cannot be uncoupled. Then these are
 932 not *coupled* processes, but are defined as *bound* processes. The electrical and chemical parts
 933 are tightly bound partial forces, since the flux cannot be partitioned but expressed only in either
 934 an electrical or chemical format, $J_{\text{H}\uparrow/e}$ or $J_{\text{H}\uparrow/n}$ (**Table 4**).

935

936 **4. Normalization: fluxes and flows**

937 The challenges of measuring mitochondrial respiratory flux are matched by those of
 938 normalization, whereby O_2 consumption may be considered as the numerator and normalization
 939 as the complementary denominator, which are tightly linked in reporting the measurements in
 940 a format commensurate with the requirements of a database.

941

942 *4.1. Flux per chamber volume*

943 When the reactor volume does not change during the reaction, which is typical for liquid
 944 phase reactions, the volume-specific *flux of a chemical reaction* r is the time derivative of the
 945 advancement of the reaction per unit volume, $J_{V,B} = d_r\check{c}_B/dt \cdot V^{-1}$ $[(\text{mol}\cdot\text{s}^{-1})\cdot\text{L}^{-1}]$. The *rate of*
 946 *concentration change* is dc_B/dt $[(\text{mol}\cdot\text{L}^{-1})\cdot\text{s}^{-1}]$, where concentration is $c_B = n_B/V$. It is helpful to
 947 make the subtle distinction between $[\text{mol}\cdot\text{s}^{-1}\cdot\text{L}^{-1}]$ and $[\text{mol}\cdot\text{L}^{-1}\cdot\text{s}^{-1}]$ for the fundamentally

948 different quantities of volume-specific flux and rate of concentration change, which merge to a
949 single expression only in closed systems. In open systems, external fluxes (such as O₂ supply)
950 are distinguished from internal transformations (metabolic flux, O₂ consumption). In a closed
951 system, external flows of all substances are zero and O₂ consumption (internal flow), I_{O_2}
952 [pmol·s⁻¹], causes a decline of the amount of O₂ in the system, n_{O_2} [nmol]. Normalization of
953 these quantities for the volume of the system, V [L = dm³], yields volume-specific O₂ flux, J_{V,O_2}
954 = I_{O_2}/V [nmol·s⁻¹·L⁻¹], and O₂ concentration, [O₂] or $c_{O_2} = n_{O_2}/V$ [nmol·mL⁻¹ = μmol·L⁻¹ = μM].
955 Instrumental background O₂ flux is due to external flux into a non-ideal closed respirometer,
956 such that total volume-specific flux has to be corrected for instrumental background O₂ flux,
957 *i.e.* O₂ diffusion into or out of the instrumental chamber. J_{V,O_2} is relevant mainly for
958 methodological reasons and should be compared with the accuracy of instrumental resolution
959 of background-corrected flux, *e.g.* ±1 nmol·s⁻¹·L⁻¹ (Gnaiger 2001). ‘Metabolic’ or catabolic
960 indicates O₂ flux, $J_{O_2,k}$, corrected for instrumental background O₂ flux and chemical background
961 O₂ flux due to autoxidation of chemical components added to the incubation medium.

962

963 4.2. System-specific and sample-specific normalization

964 Application of common and generally defined units is required for direct transfer of
965 reported results into a database. The second [s] is the *SI* unit for the base quantity *time*. It is also
966 the standard time-unit used in solution chemical kinetics. **Table 6** lists some conversion factors
967 to obtain *SI* units. The term *rate* is not sufficiently defined to be useful for a database (**Fig. 7**).
968 The inconsistency of the meanings of rate becomes fully apparent when considering Galileo
969 Galilei’s famous principle, that ‘bodies of different weight all fall at the same rate (have a
970 constant acceleration)’ (Coopersmith 2010).

971 **Extensive quantities:** An extensive quantity increases proportionally with system size.

972 The magnitude of an extensive quantity is completely additive for non-interacting subsystems,

973 such as mass or flow expressed per defined system. The magnitude of these quantities depends
 974 on the extent or size of the system (Cohen *et al.* 2008).

975 **Size-specific quantities:** ‘The adjective *specific* before the name of an extensive quantity
 976 is often used to mean *divided by mass*’ (Cohen *et al.* 2008). Mass-specific flux is flow divided
 977 by mass of the system. A mass-specific quantity is independent of the extent of non-interacting
 978 homogenous subsystems. Tissue-specific quantities are of fundamental interest in comparative
 979 mitochondrial physiology, where *specific* refers to the *type* rather than *mass* of the tissue. The
 980 term *specific*, therefore, must be further clarified, such that tissue mass-specific, *e.g.*, muscle
 981 mass-specific quantities are defined.

982

983 **Fig. 7. Different meanings of rate**

984 **may lead to confusion, if the**

985 **normalization is not sufficiently**

986 **specified.** Results are frequently

987 expressed as mass-specific flux, J_m ,

988 per mg protein, dry or wet weight

989 (mass). Cell volume, V_{cell} , or

990 mitochondrial volume, V_{mt} , may be

991 used for normalization (volume-

992 specific flux, $J_{V_{\text{cell}}}$ or $J_{V_{\text{mt}}}$), which then must be clearly distinguished from flux, J_V , expressed for

993 methodological reasons per volume of the measurement system, or flow per cell, I_x .

994

995 **Molar quantities:** ‘The adjective *molar* before the name of an extensive quantity

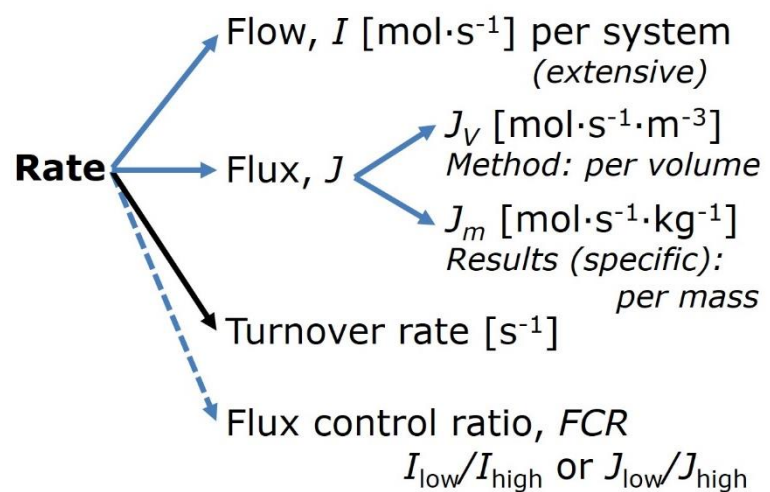
996 generally means *divided by amount of substance*’ (Cohen *et al.* 2008). The notion that all molar

997 quantities then become *intensive* causes ambiguity in the meaning of *molar Gibbs energy*. It is

998 important to emphasize the fundamental difference between normalization for amount of

999 substance *in a system* or for amount of motive substance *in a transformation*. When the Gibbs

1000 energy of a system, G [J], is divided by the amount of substance B in the system, n_B [mol], a



1001 *size-specific* molar quantity is obtained, $G_B = G/n_B$ [$\text{J}\cdot\text{mol}^{-1}$], which is not any force at all. In
 1002 contrast, when the partial Gibbs energy change, ∂G [J], is divided by the motive amount of
 1003 substance B in reaction r (advancement of reaction), $\partial_r \zeta_B$ [mol], the resulting intensive molar
 1004 quantity, $F_{B,r} = \partial G / \partial_r \zeta_B$ [$\text{J}\cdot\text{mol}^{-1}$], is the chemical motive force of reaction r involving 1 mol B
 1005 (**Table 5**, Note 4).

1006 **Flow per system, I :** In analogy to electrical terms, flow as an extensive quantity (I ; per
 1007 system) is distinguished from flux as a size-specific quantity (J ; per system size) (**Fig. 7**).
 1008 Electric current is flow, I_{el} [$\text{A} = \text{C}\cdot\text{s}^{-1}$] per system (extensive quantity). When dividing this
 1009 extensive quantity by system size (membrane area), a size-specific quantity is obtained, which
 1010 is electric flux (electric current density), J_{el} [$\text{A}\cdot\text{m}^{-2} = \text{C}\cdot\text{s}^{-1}\cdot\text{m}^{-2}$].

1011 **Size-specific flux, J :** Metabolic O_2 flow per tissue increases as tissue mass is increased.
 1012 Tissue mass-specific O_2 flux should be independent of the size of the tissue sample studied in
 1013 the instrument chamber, but volume-specific O_2 flux (per volume of the instrument chamber,
 1014 V) should increase in direct proportion to the amount of sample in the chamber. Accurate
 1015 definition of the experimental system is decisive: whether the experimental chamber is the
 1016 closed, open, isothermal or non-isothermal *system* with defined volume as part of the
 1017 measurement apparatus, in contrast to the experimental *sample* in the chamber (**Table 6**).
 1018 Volume-specific O_2 flux depends on mass-concentration of the sample in the chamber, but
 1019 should be independent of the chamber volume. There are practical limitations to increasing the
 1020 mass-concentration of the sample in the chamber, when one is concerned about crowding
 1021 effects and instrumental time resolution.

1022 **Sample concentration C_{mX} :** Normalization for sample concentration is required for
 1023 reporting respiratory data. Consider a tissue or cells as the sample, X , and the sample mass, m_X
 1024 [mg] from which a mitochondrial preparation is obtained. The sample mass, m_X , is frequently
 1025 measured as wet or dry weight, W_w or W_d [mg], or as amount of tissue or cell protein, m_{Protein} .
 1026 In the case of permeabilized tissues, cells, and homogenates, the sample concentration, $C_{mX} =$

1027 m_X/V [$\text{mg}\cdot\text{mL}^{-1} = \text{g}\cdot\text{L}^{-1}$], is simply the mass of the subsample of tissue that is transferred into
 1028 the instrument chamber. Part of the mitochondria from the tissue is lost during preparation of
 1029 isolated mitochondria, and only a fraction of mitochondria is obtained, expressed as the
 1030 mitochondrial yield (**Fig. 8**). At a high mitochondrial yield the sample of isolated mitochondria
 1031 is more representative of the total mitochondrial population than in preparations characterized
 1032 by low mitochondrial yield. Determination of the mitochondrial yield is based on measurement
 1033 of the concentration of a mitochondrial marker in the tissue homogenate, $C_{\text{mte,thom}}$, which
 1034 simultaneously provides information on the specific mitochondrial density in the sample (**Fig.**
 1035 **8**).

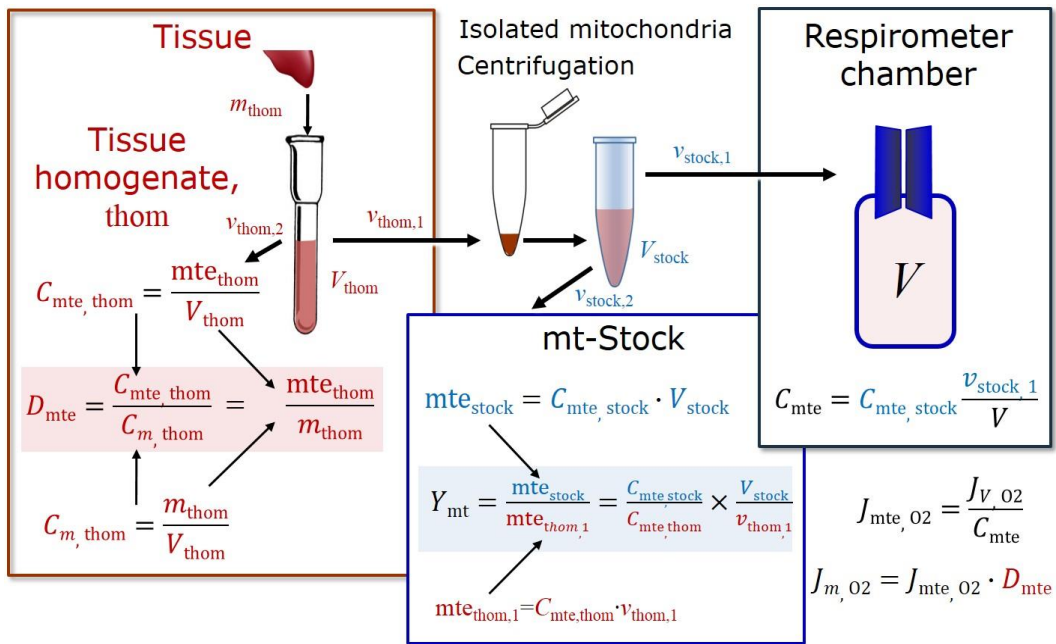
1036

1037 **Table 6. Sample concentrations and normalization of flux with SI base units.**

Expression	Symbol	Definition	SI Unit	Notes
Sample				
Identity of sample	X	Cells, animals, patients		
Number of sample entities X	N_X	Number of cells, <i>etc.</i>	x	
Mass of sample X	m_X		kg	1
Mass of entity X	M_X	$M_X = m_X \cdot N_X^{-1}$	$\text{kg}\cdot\text{x}^{-1}$	1
Mitochondria				
Mitochondria	mt	$X = \text{mt}$		
Amount of mt-elements	mte	Quantity of mt-marker	x_{mte}	
Concentrations				
Sample number concentration	C_{NX}	$C_{NX} = N_X \cdot V^{-1}$	$\text{x}\cdot\text{m}^{-3}$	2
Sample mass concentration	C_{mX}	$C_{mX} = m_X \cdot V^{-1}$	$\text{kg}\cdot\text{m}^{-3}$	
Mitochondrial concentration	C_{mte}	$C_{\text{mte}} = \text{mte} \cdot V^{-1}$	$x_{\text{mte}}\cdot\text{m}^{-3}$	3
Specific mitochondrial density	D_{mte}	$D_{\text{mte}} = \text{mte} \cdot m_X^{-1}$	$x_{\text{mte}}\cdot\text{kg}^{-1}$	4
Mitochondrial content, mte per entity X	mte_X	$\text{mte}_X = \text{mte} \cdot N_X^{-1}$	$x_{\text{mte}}\cdot\text{x}^{-1}$	5
O₂ flow and flux				
Flow	I_{O_2}	Internal flow	$\text{mol}\cdot\text{s}^{-1}$	6
Volume-specific flux	J_{V,O_2}	$J_{V,\text{O}_2} = I_{\text{O}_2} \cdot V^{-1}$	$\text{mol}\cdot\text{s}^{-1}\cdot\text{m}^{-3}$	7
Flow per sample entity X	I_{X,O_2}	$I_{X,\text{O}_2} = J_{V,\text{O}_2} \cdot C_{NX}^{-1}$	$\text{mol}\cdot\text{s}^{-1}\cdot\text{x}^{-1}$	8
Mass-specific flux	J_{mX,O_2}	$J_{mX,\text{O}_2} = J_{V,\text{O}_2} \cdot C_{mX}^{-1}$	$\text{mol}\cdot\text{s}^{-1}\cdot\text{kg}^{-1}$	9
Mitochondria-specific flux	$J_{\text{mte},\text{O}_2}$	$J_{\text{mte},\text{O}_2} = J_{V,\text{O}_2} \cdot C_{\text{mte}}^{-1}$	$\text{mol}\cdot\text{s}^{-1}\cdot x_{\text{mte}}^{-1}$	10

1039

- 1040 1 The SI prefix k is used for the SI base unit of mass (kg = 1,000 g). In praxis, various SI prefixes are
 1041 used for convenience, to make numbers easily readable, e.g. 1 mg tissue, cell or mitochondrial mass
 1042 instead of 0.000001 kg.
- 1043 2 In case $X = \text{cells}$, the sample number concentration is $C_{N_{\text{cell}}} = N_{\text{cell}} \cdot V^{-1}$, and volume may be expressed
 1044 in [$\text{dm}^3 = \text{L}$] or [$\text{cm}^3 = \text{mL}$]. See **Table 7** for different sample types.
- 1045 3 mt-concentration is an experimental variable, dependent on sample concentration: (1) $C_{\text{mte}} = \text{mte} \cdot V^{-1}$;
 1046 (2) $C_{\text{mte}} = \text{mte}_X \cdot C_{NX}$; (3) $C_{\text{mte}} = C_{mX} \cdot D_{\text{mte}}$.
- 1047 4 If the amount of mitochondria, mte, is expressed as mitochondrial mass, then D_{mte} is the mass
 1048 fraction of mitochondria in the sample. If mte is expressed as mitochondrial volume, V_{mt} , and the
 1049 mass of sample, m_X , is replaced by volume of sample, V_X , then D_{mte} is the volume fraction of
 1050 mitochondria in the sample.
- 1051 5 $\text{mte}_X = \text{mte} \cdot N_X^{-1} = C_{\text{mte}} \cdot C_{NX}^{-1}$.
- 1052 6 O_2 can be replaced by other chemicals B to study different reactions, e.g. ATP, H_2O_2 , or
 1053 compartmental translocations, e.g. Ca^{2+} .
- 1054 7 l_{O_2} and V are defined per instrument chamber as a system of constant volume (and constant
 1055 temperature), which may be closed or open. l_{O_2} is abbreviated for $l_{\text{O}_2,r}$, i.e. the metabolic or internal
 1056 O_2 flow of the chemical reaction r in which O_2 is consumed, hence the negative stoichiometric
 1057 number, $\nu_{\text{O}_2} = -1$. $l_{\text{O}_2,r} = d_r n_{\text{O}_2} / dt \cdot \nu_{\text{O}_2}^{-1}$. If r includes all chemical reactions in which O_2 participates,
 1058 then $d_r n_{\text{O}_2} = dn_{\text{O}_2} - d_e n_{\text{O}_2}$, where dn_{O_2} is the change in the amount of O_2 in the instrument chamber
 1059 and $d_e n_{\text{O}_2}$ is the amount of O_2 added externally to the system. At steady state, by definition $dn_{\text{O}_2} = 0$,
 1060 hence $d_r n_{\text{O}_2} = -d_e n_{\text{O}_2}$.
- 1061 8 J_{V,O_2} is an experimental variable, expressed per volume of the instrument chamber.
- 1062 9 l_{X,O_2} is a physiological variable, depending on the size of entity X.
- 1063 10 There are many ways to normalize for a mitochondrial marker, that are used in different experimental
 1064 approaches: (1) $J_{\text{mte},\text{O}_2} = J_{V,\text{O}_2} \cdot C_{\text{mte}}^{-1}$; (2) $J_{\text{mte},\text{O}_2} = J_{V,\text{O}_2} \cdot C_{mX}^{-1} \cdot D_{\text{mte}}^{-1} = J_{mX,\text{O}_2} \cdot D_{\text{mte}}^{-1}$; (3) $J_{\text{mte},\text{O}_2} =$
 1065 $J_{V,\text{O}_2} \cdot C_{NX}^{-1} \cdot \text{mte}_X^{-1} = l_{X,\text{O}_2} \cdot \text{mte}_X^{-1}$; (4) $J_{\text{mte},\text{O}_2} = l_{\text{O}_2} \cdot \text{mte}^{-1}$.
- 1066
- 1067



1068

Symbol	Definition [Units]
C_{mte}	Mitochondrial concentration in chamber [$x_{mte} \cdot L^{-1}$]
C_m	Sample mass concentration in chamber [$g \cdot L^{-1}$]
D_{mte}	Specific mte-density per tissue mass [$x_{mte} \cdot g^{-1}$]
J_{m,O_2}	Mass-specific O_2 flux [$nmol \cdot s^{-1} \cdot g^{-1}$]
J_{mte,O_2}	Mitochondria-specific O_2 flux [$nmol \cdot s^{-1} \cdot x_{mte}^{-1}$]
mte	Amount of mitochondrial elements [x_{mte}]
m_{thom}	Mass of tissue in the homogenate [g]
Y_{mt}	Yield of isolated mitochondria

1069

1070

1071

1072

1073

1074

1075

1076

1077

1078

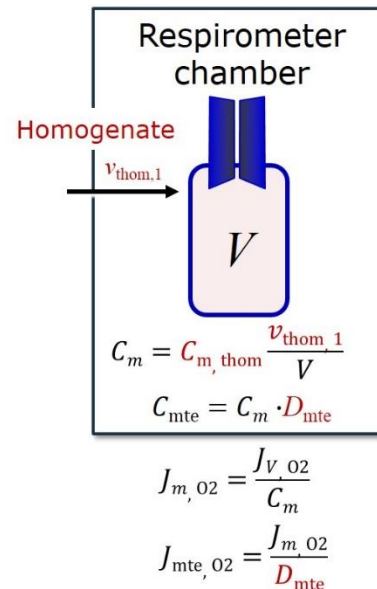


Fig. 8. Normalization of volume-specific flux of isolated mitochondria and tissue

homogenate. A: Mitochondrial yield, Y_{mt} , in preparation of isolated mitochondria. $v_{thom,1}$

and $v_{stock,1}$ are the volumes transferred from the total volume, V_{thom} and V_{stock} , respectively.

$mte_{thom,1}$ is the amount of mitochondrial elements in volume $v_{thom,1}$ used for isolation. **B:**

In respirometry with homogenate, $v_{thom,1}$ is transferred directly into the respirometer

chamber. See **Table 6** for further explanation of symbols.

1079
1080

**Table 7. Some useful abbreviations
of various sample types, X.**

Identity of sample	X
Mitochondrial preparation	mtprep
Isolated mitochondria	imt
Tissue homogenate	thom
Permeabilized tissue	pti
Permeabilized fibre	pfi
Permeabilized cell	pce
Cell	ce
Organism	org

1081

1082 Tissues can contain multiple cell populations which may have distinct mitochondrial
1083 subtypes. Mitochondria are also in a constant state of flux due to highly dynamic fission and
1084 fusion cycles, and can exist in multiple stages and sizes which may be altered by a range of
1085 factors. The isolation of mitochondria (often achieved through differential centrifugation) can
1086 therefore yield a subsample of the mitochondrial types present in a tissue, dependent on
1087 isolation protocols utilized (*e.g.* centrifugation speed). This possible artefact should be taken
1088 into account when planning experiments using isolated mitochondria. The tendency for
1089 mitochondria of specific sizes to be enriched at different centrifugation speeds also has the
1090 potential to allow the isolation of specific mitochondrial subpopulations and therefore the
1091 analysis of mitochondria from multiple cell lineages within a single tissue.

1092 **Mass-specific flux, J_{mX,O_2} :** Mass-specific flux is obtained by expressing respiration per
1093 mass of sample, m_X [mg]. X is the type of sample, *e.g.*, tissue homogenate, permeabilized fibres
1094 or cells. Volume-specific flux is divided by mass concentration of X , $J_{mX,O_2} = J_{V,O_2}/C_{mX}$; or flow
1095 per cell is divided by mass per cell, $J_{mcell,O_2} = I_{cell,O_2}/M_{cell}$. If mass-specific O_2 flux is constant
1096 and independent of sample size (expressed as mass), then there is no interaction between the
1097 subsystems. A 1.5 mg and a 3.0 mg muscle sample respire at identical mass-specific flux.

1098 Mass-specific O₂ flux, however, may change with the mass of a tissue sample, cells or isolated
 1099 mitochondria in the measuring chamber, in which case the nature of the interaction becomes an
 1100 issue. Optimization of cell density and arrangement is generally important and particularly in
 1101 experiments carried out in wells, considering the confluency of the cell monolayer or clumps
 1102 of cells (Salabei *et al.* 2014).

1103 **Number concentration, C_{NX} :** The experimental *number concentration* of sample in the
 1104 case of cells or animals, *e.g.*, nematodes is $C_{NX} = N_X/V$ [$x \cdot \text{mL}^{-1}$], where N_X is the number of
 1105 cells or organisms in the chamber (**Table 6**).

1106 **Flow per sample entity, I_{X,O_2} :** A special case of normalization is encountered in
 1107 respiratory studies with permeabilized (or intact) cells. If respiration is expressed per cell, the
 1108 O₂ flow per measurement system is replaced by the O₂ flow per cell, I_{cell,O_2} (**Table 6**). O₂ flow
 1109 can be calculated from volume-specific O₂ flux, J_{V,O_2} [$\text{nmol} \cdot \text{s}^{-1} \cdot \text{L}^{-1}$] (per V of the measurement
 1110 chamber [L]), divided by the number concentration of cells, $C_{N_{ce}} = N_{ce}/V$ [$\text{cell} \cdot \text{L}^{-1}$], where N_{ce}
 1111 is the number of cells in the chamber. Cellular O₂ flow can be compared between cells of
 1112 identical size. To take into account changes and differences in cell size, further normalization
 1113 is required to obtain cell size-specific or mitochondrial marker-specific O₂ flux (Renner *et al.*
 1114 2003).

1115 The complexity changes when the sample is a whole organism studied as an experimental
 1116 model. The well-established scaling law in respiratory physiology reveals a strong interaction
 1117 of O₂ consumption and individual body mass of an organism, since *basal* metabolic rate (flow)
 1118 does not increase linearly with body mass, whereas *maximum* mass-specific O₂ flux, $\dot{V}_{O_{2\text{max}}}$ or
 1119 $\dot{V}_{O_{2\text{peak}}}$, is approximately constant across a large range of individual body mass (Weibel and
 1120 Hoppeler 2005), with individuals, breeds, and certain species deviating substantially from this
 1121 general relationship. $\dot{V}_{O_{2\text{peak}}}$ of human endurance athletes is 60 to 80 mL O₂ · min⁻¹ · kg⁻¹ body
 1122 mass, converted to $J_{m,O_{2\text{peak}}}$ of 45 to 60 nmol · s⁻¹ · g⁻¹ (Gnaiger 2014; **Table 8**).

1123

1124 4.3. Normalization for mitochondrial content

1125 Normalization is a problematic subject and it is essential to consider the question of the
1126 study. If the study aims to compare tissue performance, such as the effects of a certain treatment
1127 on a specific tissue, then normalization can be successful, using tissue mass or protein content,
1128 for example. If the aim, however, is to find differences of mitochondrial function independent
1129 of mitochondrial density (**Table 6**), then normalization to a mitochondrial marker is imperative
1130 (**Fig. 9**). However, one cannot assume that quantitative changes in various markers such as
1131 mitochondrial proteins necessarily occur in parallel with one another. It is important to first
1132 establish that the marker chosen is not selectively altered by the performed treatment. In
1133 conclusion, the normalization must reflect the question under investigation to reach a satisfying
1134 answer. On the other hand, the goal of comparing results across projects and institutions
1135 requires some standardization on normalization for entry into a databank.

1136 **Mitochondrial concentration, C_{mte} , and mitochondrial markers:** It is important that
1137 mitochondrial concentration in the tissue and the measurement chamber be quantified, as a
1138 physiological output and result of mitochondrial biogenesis and degradation, and as a quantity
1139 for normalization in functional analyses. Mitochondrial organelles comprise a cellular
1140 reticulum that is in a continual flux of fusion and fission. Hence the definition of an "amount"
1141 of mitochondria is often misconceived: mitochondria cannot be counted as a number of
1142 occurring elements. Therefore, quantification of the "amount" of mitochondria depends on
1143 measurement of chosen mitochondrial markers. 'Mitochondria are the structural and functional
1144 elemental units of cell respiration' (Gnaiger 2014). The quantity of a mitochondrial marker can
1145 be considered as the measurement of the amount of *elemental mitochondrial units* or
1146 *mitochondrial elements*, mte. However, since mitochondrial quality changes under certain
1147 stimuli, particularly in mitochondrial dysfunction and after exercise training (Pesta *et al.* 2011;
1148 Campos *et al.* 2017), some markers can vary while other markers are unchanged. (I)
1149 Mitochondrial volume and membrane area are structural markers, whereas mitochondrial

1150 protein mass is frequently used as a marker for isolated mitochondria. (2) Molecular and
 1151 enzymatic mitochondrial markers (amounts or activities) can be selected as matrix markers,
 1152 *e.g.*, citrate synthase activity, mtDNA; mtIM-markers, *e.g.*, cytochrome *c* oxidase activity, *aa₃*
 1153 content, cardiolipin, or mtOM-markers, *e.g.*, TOM20. (3) Extending the measurement of
 1154 mitochondrial marker enzyme activity to mitochondrial pathway capacity, measured as ET- or
 1155 OXPHOS-capacity, can be considered as an integrative functional mitochondrial marker.

1156 Depending on the type of mitochondrial marker, the mitochondrial elements, *mte*, are
 1157 expressed in marker-specific units. Although concentration and density are used synonymously
 1158 in physical chemistry, it is recommended to distinguish *experimental mitochondrial*
 1159 *concentration*, $C_{mte} = mte/V$ and *physiological mitochondrial density*, $D_{mte} = mte/m_X$. Then
 1160 mitochondrial density is the amount of mitochondrial elements per mass of tissue (**Fig. 9**). The
 1161 former is mitochondrial density multiplied by sample mass concentration, $C_{mte} = D_{mte} \cdot C_{mX}$, or
 1162 mitochondrial content multiplied by sample number concentration, $C_{mte} = mte_X \cdot C_{NX}$ (**Table 6**).

1163 **Mitochondria-specific flux, J_{mte,O_2}** : Volume-specific metabolic O_2 flux depends on: (1)
 1164 the sample concentration in the volume of the instrument chamber, C_{mX} , or C_{NX} ; (2) the
 1165 mitochondrial density in the sample, $D_{mte} = mte/m_X$ or $mte_X = mte/N_X$; and (3) the specific
 1166 mitochondrial activity or performance per elemental mitochondrial unit, $J_{mte,O_2} = J_{V,O_2}/C_{mte}$
 1167 (**Table 6**). Obviously, the numerical results for J_{mte,O_2} vary according to the type of
 1168 mitochondrial marker chosen for measurement of *mte* and $C_{mte} = mte/V$.

1169

Flow, Performance	=	Element function	x	Element density	x	Size of entity
$\frac{\text{mol}\cdot\text{s}^{-1}}{x}$	=	$\frac{\text{mol}\cdot\text{s}^{-1}}{X_{\text{mte}}}$	·	$\frac{X_{\text{mte}}}{\text{kg}}$	·	$\frac{\text{kg}}{x}$

A	Flow	=	mt-specific flux	x	mt-structure, functional elements
	I_{X,O_2}	=	$J_{\text{mte},\text{O}_2}$	·	mte_X
					$\left(\frac{\text{mte}_X}{M_X} \cdot M_X \right)$

I_{X,O_2}	=	$J_{\text{mte},\text{O}_2}$	·	D_{mte}	·	M_X
$\frac{I_{X,\text{O}_2}}{M_X}$	=	$\frac{I_{X,\text{O}_2}}{\text{mte}_X}$	·	$\frac{\text{mte}_X}{M_X}$		

B	I_{X,O_2}	=	J_{mX,O_2}	·	M_X
	Flow	=	Entity mass-specific flux	x	Mass of entity

1170
 1171 **Fig. 9. Structure-function analysis of performance of an**
 1172 **organism, organ or tissue, or a cell (sample entity X). O₂**
 1173 **flow, I_{X,O_2} , is the product of performance per functional**
 1174 **element (element function, mitochondria-specific flux),**
 1175 **element density (mitochondrial density, D_{mte}), and size of**
 1176 **entity X (mass M_X). (A) Structured analysis: performance is the**
 1177 **product of mitochondrial function (mt-specific flux) and structure**
 1178 **(functional elements; D_{mte} times mass of X). (B) Unstructured**
 1179 **analysis: performance is the product of entity mass-specific flux,**
 1180 **$J_{mX,\text{O}_2} = I_{X,\text{O}_2}/M_X = I_{\text{O}_2}/m_X$ [mol·s⁻¹·kg⁻¹] and size of entity,**
 1181 **expressed as mass of X; $M_X = m_X \cdot N_X^{-1}$ [kg·x⁻¹]. See Table 6 for**
 1182 **further explanation of quantities and units. Modified from Gnaiger**
 1183 **(2014).**

1184 4.4. Evaluation of mitochondrial markers

1185 Different methods are implicated in quantification of mitochondrial markers and have
 1186 different strengths. Some problems are common for all mitochondrial markers, mte: (I)
 1187 Accuracy of measurement is crucial, since even a highly accurate and reproducible
 1188

1189 measurement of O₂ flux results in an inaccurate and noisy expression normalized for a biased
1190 and noisy measurement of a mitochondrial marker. This problem is acute in mitochondrial
1191 respiration because the denominators used (the mitochondrial markers) are often very small
1192 moieties whose accurate and precise determination is difficult. This problem can be avoided
1193 when O₂ fluxes measured in substrate-uncoupler-inhibitor titration protocols are normalized for
1194 flux in a defined respiratory reference state, which is used as an *internal* marker and yields flux
1195 control ratios, *FCRs* (Fig. 7). *FCRs* are independent of any *externally* measured markers and,
1196 therefore, are statistically very robust, considering the limitations of ratios in general (Jasienski
1197 and Bazzaz 1999). *FCRs* indicate qualitative changes of mitochondrial respiratory control, with
1198 highest quantitative resolution, separating the effect of mitochondrial density or concentration
1199 on J_{mX,O_2} and I_{X,O_2} from that of function per elemental mitochondrial marker, J_{mte,O_2} (Pesta *et*
1200 *al.* 2011; Gnaiger 2014). (2) If mitochondrial quality does not change and only the amount of
1201 mitochondria, defined by the chosen mitochondrial marker, varies as a determinant of mass-
1202 specific flux, any marker is equally qualified in principle; then in practice selection of the
1203 optimum marker depends only on the accuracy and precision of measurement of the
1204 mitochondrial marker. (3) If mitochondrial flux control ratios change, then there may not be
1205 any best mitochondrial marker. In general, measurement of multiple mitochondrial markers
1206 enables a comparison and evaluation of normalization for a variety of mitochondrial markers.
1207 Particularly during postnatal development, the activity of marker enzymes, such as cytochrome
1208 *c* oxidase and citrate synthase, follows different time courses (Drahota *et al.* 2004). Evaluation
1209 of mitochondrial markers in healthy controls is insufficient for providing guidelines for
1210 application in the diagnosis of pathological states and specific treatments.

1211 In line with the concept of the respiratory control ratio (Chance and Williams 1955a), the
1212 most readily used normalization is that of flux control ratios and flux control factors (Gnaiger
1213 2014). Selection of the state of maximum flux in a protocol as the reference state has the
1214 advantages of (1) internal normalization, (2) statistical linearization of the response in the range

1215 of 0 to 1, and (3) consideration of maximum flux for integrating a very large number of
1216 elemental steps in the OXPHOS- or ET-pathways. This reduces the risk of selecting a functional
1217 marker that is specifically altered by the treatment or pathodology, yet increases the chance that
1218 the highly integrative pathway is disproportionately affected, *e.g.* the OXPHOS- rather than
1219 ET-pathway in case of an enzymatic defect in the phosphorylation-pathway. In this case,
1220 additional information can be obtained by reporting flux control ratios based on a reference
1221 state which indicates stable tissue-mass specific flux. Stereological determination of
1222 mitochondrial content via two-dimensional transmission electron microscopy can have
1223 limitations due to the dynamics of mitochondrial size (Meinild Lundby *et al.* 2017). Accurate
1224 determination of three-dimensional volume by two-dimensional microscopy can be both time
1225 consuming and statistically challenging (Larsen *et al.* 2012). Using mitochondrial marker
1226 enzymes (citrate synthase activity, Complex I–IV amount or activity) for normalization of flux
1227 is limited in part by the same factors that apply to the use of flux control ratios. Strong
1228 correlations between various mitochondrial markers and citrate synthase activity (Reichmann
1229 *et al.* 1985; Boushel *et al.* 2007; Mogensen *et al.* 2007) are expected in a specific tissue of
1230 healthy subjects and in disease states not specifically targeting citrate synthase. Citrate synthase
1231 activity is acutely modifiable by exercise (Tonkonogi *et al.* 1997; Leek *et al.* 2001). Evaluation
1232 of mitochondrial markers related to a selected age and sex cohort cannot be extrapolated to
1233 provide recommendations for normalization in respirometric diagnosis of disease, in different
1234 states of development and ageing, different cell types, tissues, and species. mtDNA normalised
1235 to nDNA via qPCR is correlated to functional mitochondrial markers including OXPHOS- and
1236 ET-capacity in some cases (Puntschart *et al.* 1995; Wang *et al.* 1999; Menshikova *et al.* 2006;
1237 Boushel *et al.* 2007), but lack of such correlations have been reported (Menshikova *et al.* 2005;
1238 Schultz and Wiesner 2000; Pesta *et al.* 2011). Several studies indicate a strong correlation
1239 between cardiolipin content and increase in mitochondrial functionality with exercise

1240 (Menshikova *et al.* 2005; Menshikova *et al.* 2007; Larsen *et al.* 2012; Faber *et al.* 2014), but its
 1241 use as a general mitochondrial biomarker in disease remains questionable.

1242

1243 4.5. Conversion: units and normalization

1244 Many different units have been used to report the rate of oxygen consumption, OCR
 1245 (**Table 8**). *SI* base units provide the common reference for introducing the theoretical principles
 1246 (**Fig. 7**), and are used with appropriately chosen *SI* prefixes to express numerical data in the
 1247 most practical format, with an effort towards unification within specific areas of application
 1248 (**Table 9**). For studies of cells, we recommend that respiration be expressed, as far as possible,
 1249 as (1) O₂ flux normalized for a mitochondrial marker, for separation of the effects of
 1250 mitochondrial quality and content on cell respiration (this includes *FCRs* as a normalization for
 1251 a functional mitochondrial marker); (2) O₂ flux in units of cell volume or mass, for comparison
 1252 of respiration of cells with different cell size (Renner *et al.* 2003) and with studies on tissue
 1253 preparations, and (3) O₂ flow in units of attomole (10⁻¹⁸ mol) of O₂ consumed by each cell in a
 1254 second [amol·s⁻¹·cell⁻¹], numerically equivalent to [pmol·s⁻¹·10⁻⁶ cells]. This convention allows
 1255 information to be easily used when designing experiments in which oxygen consumption must
 1256 be considered. For example, to estimate the volume-specific O₂ flux in an instrument chamber
 1257 that would be expected at a particular cell number concentration, one simply needs to multiply
 1258 the flow per cell by the number of cells per volume of interest. This provides the amount of O₂
 1259 [mol] consumed per time [s⁻¹] per unit volume [L⁻¹]. At an O₂ flow of 100 amol·s⁻¹·cell⁻¹ and a
 1260 cell density of 10⁹ cells·L⁻¹ (10⁶ cells·mL⁻¹), the volume-specific O₂ flux is 100 nmol·s⁻¹·L⁻¹ (100
 1261 pmol·s⁻¹·mL⁻¹).

1262 Although volume is expressed as m³ using the *SI* base unit, the litre [dm³] is the basic unit
 1263 of volume for concentration and is used for most solution chemical kinetics. If one multiplies
 1264 $I_{\text{cell},\text{O}_2}$ by C_{Ncell} , then the result will not only be the amount of O₂ [mol] consumed per time [s⁻¹]
 1265 in one litre [L⁻¹], but also the change in the concentration of oxygen per second (for any volume

1266 of an ideally closed system). This is ideal for kinetic modeling as it blends with chemical rate
 1267 equations where concentrations are typically expressed in $\text{mol}\cdot\text{L}^{-1}$ (Wagner *et al.* 2011). In
 1268 studies of multinuclear cells, such as differentiated skeletal muscle cells, it is easy to determine
 1269 the number of nuclei but not the total number of cells. A generalized concept, therefore, is
 1270 obtained by substituting cells by nuclei as the sample entity. This does not hold, however, for
 1271 enucleated platelets.

1272

1273 4.5. Conversion: oxygen, proton and ATP flux

1274 $J_{\text{O}_2,k}$ is coupled in mitochondrial steady states to proton cycling, $J_{\text{H}^+\infty} = J_{\text{H}^+\uparrow} = J_{\text{H}^+\downarrow}$ (**Fig.**
 1275 **2**). $J_{\text{H}^+\uparrow/n}$ and $J_{\text{H}^+\downarrow/n}$ [$\text{nmol}\cdot\text{s}^{-1}\cdot\text{L}^{-1}$] are converted into electrical units, $J_{\text{H}^+\uparrow/e}$ [$\text{mC}\cdot\text{s}^{-1}\cdot\text{L}^{-1} = \text{mA}\cdot\text{L}^{-1}$]
 1276 $= J_{\text{H}^+\uparrow/n}$ [$\text{nmol}\cdot\text{s}^{-1}\cdot\text{L}^{-1}$] $\cdot F$ [$\text{C}\cdot\text{mol}^{-1}$] $\cdot 10^{-6}$ (**Table 4**). At a $J_{\text{H}^+\uparrow}/J_{\text{O}_2,k}$ ratio or $\text{H}^+\uparrow/\text{O}_2$ of 20 ($\text{H}^+\uparrow/\text{O} =$
 1277 10), a volume-specific O_2 flux of $100 \text{ nmol}\cdot\text{s}^{-1}\cdot\text{L}^{-1}$ would correspond to a proton flux of 2,000
 1278 $\text{nmol H}^+\uparrow\cdot\text{s}^{-1}\cdot\text{L}^{-1}$ or volume-specific current of $193 \text{ mA}\cdot\text{L}^{-1}$.

$$1279 \quad J_{V,\text{H}^+\uparrow/e} [\text{mA}\cdot\text{L}^{-1}] = J_{V,\text{H}^+\uparrow/n} \cdot F \cdot 10^{-6} [\text{nmol}\cdot\text{s}^{-1}\cdot\text{L}^{-1} \cdot \text{mC}\cdot\text{nmol}^{-1}] \quad (\text{Eq. 3.1})$$

$$1280 \quad J_{V,\text{H}^+\uparrow/e} [\text{mA}\cdot\text{L}^{-1}] = J_{V,\text{O}_2} \cdot (\text{H}^+\uparrow/\text{O}_2) \cdot F \cdot 10^{-6} [\text{mC}\cdot\text{s}^{-1}\cdot\text{L}^{-1} = \text{mA}\cdot\text{L}^{-1}] \quad (\text{Eq. 3.2})$$

1281 ET-capacity in various human cell types including HEK 293, primary HUVEC and fibroblasts
 1282 ranges from 50 to $180 \text{ amol}\cdot\text{s}^{-1}\cdot\text{cell}^{-1}$, measured in intact cells in the noncoupled state (see
 1283 Gnaiger 2014). At $100 \text{ amol}\cdot\text{s}^{-1}\cdot\text{cell}^{-1}$ corrected for ROX (corresponding to a catabolic power
 1284 of $-48 \text{ pW}\cdot\text{cell}^{-1}$), the current across the mt-membranes, I_e , approximates $193 \text{ pA}\cdot\text{cell}^{-1}$ or 0.2
 1285 nA per cell. See Rich (2003) for an extension of quantitative bioenergetics from the molecular
 1286 to the human scale, with a transmembrane proton flux equivalent to 520 A in an adult at a
 1287 catabolic power of -110 W. Modelling approaches illustrate the link between proton motive
 1288 force and currents (Willis *et al.* 2016). For NADH- and succinate-linked respiration, the
 1289 mechanistic $\text{P}\gg/\text{O}_2$ ratio (referring to the full 4 electron reduction of O_2) is calculated at 20/3.7
 1290 and 12/3.7, respectively (Eq. 4) equal to 5.4 and 3.3. The classical $\text{P}\gg/\text{O}$ ratios (referring to the
 1291 2 electron reduction of 0.5 O_2) are 2.7 and 1.6 (Watt *et al.* 2010), in direct agreement with the

1292 measured P \gg /O ratio for succinate of 1.58 ± 0.02 (Gnaiger *et al.* 2000; for detailed reviews see
1293 Wikström and Hummer 2012; Sazanov 2015),

$$1294 \quad P\gg/O_2 = (H^+\uparrow/O_2)/(H^+\downarrow/P\gg) \quad (\text{Eq. 4})$$

1295 In summary (**Fig. 1**),

$$1296 \quad J_{V,P\gg} [\text{nmol}\cdot\text{s}^{-1}\cdot\text{L}^{-1}] = J_{V,O_2}\cdot(H^+\uparrow/O_2)/(H^+\downarrow/P\gg) \quad (\text{Eq. 5.1})$$

$$1297 \quad J_{V,P\gg} [\text{nmol}\cdot\text{s}^{-1}\cdot\text{L}^{-1}] = J_{V,O_2}\cdot(P\gg/O_2) \quad (\text{Eq. 5.2})$$

1298

1299 **Table 8. Conversion of various units used in respirometry and**
1300 **ergometry.** e is the number of electrons or reducing equivalents. z_B is the
1301 charge number of entity B.

1302

1 Unit	x	Multiplication factor	SI-Unit	Note
ng.atom O \cdot s ⁻¹	(2 e)	0.5	nmol O ₂ \cdot s ⁻¹	
ng.atom O \cdot min ⁻¹	(2 e)	8.33	pmol O ₂ \cdot s ⁻¹	
natom O \cdot min ⁻¹	(2 e)	8.33	pmol O ₂ \cdot s ⁻¹	
nmol O ₂ \cdot min ⁻¹	(4 e)	16.67	pmol O ₂ \cdot s ⁻¹	
nmol O ₂ \cdot h ⁻¹	(4 e)	0.2778	pmol O ₂ \cdot s ⁻¹	
mL O ₂ \cdot min ⁻¹ at STPD ^a		0.744	μmol O ₂ \cdot s ⁻¹	1
W = J/s at -470 kJ/mol O ₂		-2.128	μmol O ₂ \cdot s ⁻¹	
mA = mC \cdot s ⁻¹	(z _{H+} = 1)	10.36	nmol H ⁺ \cdot s ⁻¹	2
mA = mC \cdot s ⁻¹	(z _{O2} = 4)	2.59	nmol O ₂ \cdot s ⁻¹	2
nmol H ⁺ \cdot s ⁻¹	(z _{H+} = 1)	0.09649	mA	3
nmol O ₂ \cdot s ⁻¹	(z _{O2} = 4)	0.38594	mA	3

1303

1304 1 At standard temperature and pressure dry (STPD: 0 °C = 273.15 K and 1 atm =
1305 101.325 kPa = 760 mmHg), the molar volume of an ideal gas, V_m, and V_{m,O₂} is
1306 22.414 and 22.392 L \cdot mol⁻¹ respectively. Rounded to three decimal places, both
1307 values yield the conversion factor of 0.744. For comparison at NTPD (20 °C),
1308 V_{m,O₂} is 24.038 L \cdot mol⁻¹. Note that the SI standard pressure is 100 kPa.

1309 2 The multiplication factor is $10^6/(z_B \cdot F)$.

1310 3 The multiplication factor is $z_B \cdot F/10^6$.

1311

1312 **Table 9. Conversion of units with preservation of numerical values.**

Name	Frequently used unit	Equivalent unit	Note
Volume-specific flux, J_{V,O_2}	$\text{pmol} \cdot \text{s}^{-1} \cdot \text{mL}^{-1}$ $\text{mmol} \cdot \text{s}^{-1} \cdot \text{L}^{-1}$	$\text{nmol} \cdot \text{s}^{-1} \cdot \text{L}^{-1}$ $\text{mol} \cdot \text{s}^{-1} \cdot \text{m}^{-3}$	1
Cell-specific flow, I_{O_2}	$\text{pmol} \cdot \text{s}^{-1} \cdot 10^{-6}$ cells	$\text{amol} \cdot \text{s}^{-1} \cdot \text{cell}^{-1}$	2
	$\text{pmol} \cdot \text{s}^{-1} \cdot 10^{-9}$ cells	$\text{zmol} \cdot \text{s}^{-1} \cdot \text{cell}^{-1}$	3
Cell number concentration, C_{Nce}	10^6 cells $\cdot \text{mL}^{-1}$	10^9 cells $\cdot \text{L}^{-1}$	
Mitochondrial protein concentration, C_{mte}	$0.1 \text{ mg} \cdot \text{mL}^{-1}$	$0.1 \text{ g} \cdot \text{L}^{-1}$	
Mass-specific flux, J_{m,O_2}	$\text{pmol} \cdot \text{s}^{-1} \cdot \text{mg}^{-1}$	$\text{nmol} \cdot \text{s}^{-1} \cdot \text{g}^{-1}$	4
Catabolic power, $P_{O_2,k}$	$\mu\text{W} \cdot 10^{-6}$ cells	$\text{pW} \cdot \text{cell}^{-1}$	1
Volume	1,000 L	m^3 (1,000 kg)	
	L	dm^3 (kg)	
	mL	cm^3 (g)	
	μL	mm^3 (mg)	
	fL	μm^3 (pg)	5
Amount of substance concentration	$\text{M} = \text{mol} \cdot \text{L}^{-1}$	$\text{mol} \cdot \text{dm}^{-3}$	

1313

1314 1 pmol: picomole = 10^{-12} mol

1315 2 amol: attomole = 10^{-18} mol

1316 3 zmol: zeptomole = 10^{-21} mol

1317 4 nmol: nanomole = 10^{-9} mol

1318 5 1 fL = 10^{-15} L

1319

1320 We consider isolated mitochondria as powerhouses and proton pumps as molecular
 1321 machines to relate experimental results to energy metabolism of the intact cell. The cellular
 1322 P_{\gg}/O_2 based on oxidation of glycogen is increased by the glycolytic (fermentative) substrate-
 1323 level phosphorylation of 3 P_{\gg}/Glyc , *i.e.*, 0.5 mol P_{\gg} for each mol O_2 consumed in the complete
 1324 oxidation of a mol glycosyl unit (Glyc). Adding 0.5 to the mitochondrial P_{\gg}/O_2 ratio of 5.4
 1325 yields a bioenergetic cell physiological P_{\gg}/O_2 ratio close to 6. Two NADH equivalents are
 1326 formed during glycolysis and transported from the cytosol into the mitochondrial matrix, either
 1327 by the malate-aspartate shuttle or by the glycerophosphate shuttle resulting in different
 1328 theoretical yield of ATP generated by mitochondria, the energetic cost of which potentially
 1329 must be taken into account. Considering also substrate-level phosphorylation in the TCA cycle,

1330 this high P_{H}/O_2 ratio not only reflects proton translocation and OXPHOS studied in isolation,
1331 but integrates mitochondrial physiology with energy transformation in the living cell (Gnaiger
1332 1993a).

1333

1334 **5. Conclusions**

1335 MitoEAGLE can serve as a gateway to better diagnose mitochondrial respiratory defects
1336 linked to genetic variation, age-related health risks, sex-specific mitochondrial performance,
1337 lifestyle with its effects on degenerative diseases, and thermal and chemical environment. The
1338 present recommendations on coupling control states and rates, linked to the concept of the
1339 protonmotive force (Part 1) will be extended in a series of reports on pathway control of
1340 mitochondrial respiration, respiratory states in intact cells, and harmonization of experimental
1341 procedures.

1342

1343 **Box 5: Mitochondrial and cell respiration**

1344 Mitochondrial and cell respiration is the process of highly exergonic and exothermic energy
1345 transformation in which scalar redox reactions are coupled to vectorial ion translocation across
1346 a semipermeable membrane, which separates the small volume of a bacterial cell or
1347 mitochondrion from the larger volume of its surroundings. The electrochemical exergy can be
1348 partially conserved in the phosphorylation of ADP to ATP or in ion pumping, or dissipated in
1349 an electrochemical short-circuit. Respiration is thus clearly distinguished from fermentation as
1350 the counterpart of cellular core energy metabolism. Respiration is separated in mitochondrial
1351 preparations from the partial contribution of fermentative pathways of the intact cell. According
1352 to this definition, residual oxygen consumption, as measured after inhibition of mitochondrial
1353 electron transfer, does not belong to the class of catabolic reactions and is, therefore, subtracted
1354 from total oxygen consumption to obtain baseline-corrected respiration.

1355

1356 The optimal choice for expressing mitochondrial and cell respiration (**Box 5**) as O₂ flow
1357 per biological system, and normalization for specific tissue-markers (volume, mass, protein)
1358 and mitochondrial markers (volume, protein, content, mtDNA, activity of marker enzymes,
1359 respiratory reference state) is guided by the scientific question under study. Interpretation of
1360 the obtained data depends critically on appropriate normalization, and therefore reporting rates
1361 merely as nmol·s⁻¹ is discouraged, since it restricts the analysis to intra-experimental
1362 comparison of relative (qualitative) differences. Expressing O₂ consumption per cell may not
1363 be possible when dealing with tissues. For studies with mitochondrial preparations, we
1364 recommend that normalizations be provided as far as possible: (1) on a per cell basis as O₂ flow
1365 (a biophysical normalization); (2) per g cell or tissue protein, or per cell or tissue mass as mass-
1366 specific O₂ flux (a cellular normalization); and (3) per mitochondrial marker as mt-specific flux
1367 (a mitochondrial normalization). With information on cell size and the use of multiple
1368 normalizations, maximum potential information is available (Renner *et al.* 2003; Wagner *et al.*
1369 2011; Gnaiger 2014). When using isolated mitochondria, mitochondrial protein is a frequently
1370 applied mitochondrial marker, the use of which is basically restricted to isolated mitochondria.
1371 Mitochondrial markers, such as citrate synthase activity as an enzymatic matrix marker, provide
1372 a link to the tissue of origin on the basis of calculating the mitochondrial yield, *i.e.*, the fraction
1373 of mitochondrial marker obtained from a unit mass of tissue.

1374

1375 **Acknowledgements**

1376 We thank M. Beno for management assistance. Supported by COST Action CA15203
1377 MitoEAGLE and K-Regio project MitoFit (EG).

1378 **Competing financial interests:** E.G. is founder and CEO of Oroboros Instruments, Innsbruck,
1379 Austria.

1380

1381

- 1382 **6. References** (*incomplete; www links will be deleted in the final version*)
- 1383 Altmann R (1894) Die Elementarorganismen und ihre Beziehungen zu den Zellen. Zweite
1384 vermehrte Auflage. Verlag Von Veit & Comp, Leipzig:160 pp. -
1385 www.mitoeagle.org/index.php/Altmann_1894_Verlag_Von_Veit_%26_Comp
- 1386 Beard DA (2005) A biophysical model of the mitochondrial respiratory system and oxidative
1387 phosphorylation. PLoS Comput Biol 1(4):e36. -
1388 http://www.mitoeagle.org/index.php/Beard_2005_PLOS_Comput_Biol
- 1389 Birkedal R, Laasmaa M, Vendelin M (2014) The location of energetic compartments affects
1390 energetic communication in cardiomyocytes. Front Physiol 5:376. doi:
1391 10.3389/fphys.2014.00376. eCollection 2014. PMID: 25324784
- 1392 Breton S, Beaupré HD, Stewart DT, Hoeh WR, Blier PU (2007) The unusual system of
1393 doubly uniparental inheritance of mtDNA: isn't one enough? Trends Genet 23:465-74.
- 1394 Brown GC (1992) Control of respiration and ATP synthesis in mammalian mitochondria and
1395 cells. Biochem J 284:1-13. - www.mitoeagle.org/index.php/Brown_1992_Biochem_J
- 1396 Campos JC, Queliconi BB, Bozi LHM, Bechara LRG, Dourado PMM, Andres AM, Jannig
1397 PR, Gomes KMS, Zambelli VO, Rocha-Resende C, Guatimosim S, Brum PC, Mochly-
1398 Rosen D, Gottlieb RA, Kowaltowski AJ, Ferreira JCB (2017) Exercise reestablishes
1399 autophagic flux and mitochondrial quality control in heart failure. Autophagy 13:1304-
1400 317.
- 1401 Chance B, Williams GR (1955a) Respiratory enzymes in oxidative phosphorylation. I.
1402 Kinetics of oxygen utilization. J Biol Chem 217:383-93. -
1403 http://www.mitoeagle.org/index.php/Chance_1955_J_Biol_Chem-I
- 1404 Chance B, Williams GR (1955b) Respiratory enzymes in oxidative phosphorylation: III. The
1405 steady state. J Biol Chem 217:409-27. -
1406 www.mitoeagle.org/index.php/Chance_1955_J_Biol_Chem-III

- 1407 Chance B, Williams GR (1955c) Respiratory enzymes in oxidative phosphorylation. IV. The
1408 respiratory chain. *J Biol Chem* 217:429-38. -
1409 www.mitoeagle.org/index.php/Chance_1955_J_Biol_Chem-IV
- 1410 Chance B, Williams GR (1956) The respiratory chain and oxidative phosphorylation. *Adv*
1411 *Enzymol Relat Subj Biochem* 17:65-134. -
1412 www.mitoeagle.org/index.php/Chance_1956_Adv_Enzymol_Relat_Subj_Biochem
- 1413 Cobb LJ, Lee C, Xiao J, Yen K, Wong RG, Nakamura HK, Mehta HH, Gao Q, Ashur C,
1414 Huffman DM, Wan J, Muzumdar R, Barzilai N, Cohen P (2016) Naturally occurring
1415 mitochondrial-derived peptides are age-dependent regulators of apoptosis, insulin
1416 sensitivity, and inflammatory markers. *Aging (Albany NY)* 8:796-809.
- 1417 Cohen ER, Cvitas T, Frey JG, Holmström B, Kuchitsu K, Marquardt R, Mills I, Pavese F,
1418 Quack M, Stohner J, Strauss HL, Takami M, Thor HL (2008) Quantities, units and
1419 symbols in physical chemistry, IUPAC Green Book, 3rd Edition, 2nd Printing, IUPAC &
1420 RSC Publishing, Cambridge. -
1421 www.mitoeagle.org/index.php/Cohen_2008_IUPAC_Green_Book
- 1422 Cooper H, Hedges LV, Valentine JC, eds (2009) The handbook of research synthesis and
1423 meta-analysis. Russell Sage Foundation.
- 1424 Coopersmith J (2010) Energy, the subtle concept. The discovery of Feynman's blocks from
1425 Leibnitz to Einstein. Oxford University Press:400 pp.
- 1426 Cummins J (1998) Mitochondrial DNA in mammalian reproduction. *Rev Reprod* 3:172-82.
- 1427 Dai Q, Shah AA, Garde RV, Yonish BA, Zhang L, Medvitz NA, Miller SE, Hansen EL, Dunn
1428 CN, Price TM (2013) A truncated progesterone receptor (PR-M) localizes to the
1429 mitochondrion and controls cellular respiration. *Mol Endocrinol* 27:741-53.
- 1430 Divakaruni AS, Brand MD (2011) The regulation and physiology of mitochondrial proton
1431 leak. *Physiology (Bethesda)* 26:192-205.

- 1432 Drahota Z, Milerová M, Stieglerová A, Houstek J, Ostádal B (2004) Developmental changes
1433 of cytochrome *c* oxidase and citrate synthase in rat heart homogenate. *Physiol Res*
1434 53:119-22.
- 1435 Duarte FV, Palmeira CM, Rolo AP (2014) The role of microRNAs in mitochondria: small
1436 players acting wide. *Genes (Basel)* 5:865-86.
- 1437 Dufour S, Rousse N, Canioni P, Diolez P (1996) Top-down control analysis of temperature
1438 effect on oxidative phosphorylation. *Biochem J* 314:743-51.
- 1439 Ernster L, Schatz G (1981) Mitochondria: a historical review. *J Cell Biol* 91:227s-55s. -
1440 www.mitoeagle.org/index.php/Ernster_1981_J_Cell_Biol
- 1441 Estabrook RW (1967) Mitochondrial respiratory control and the polarographic measurement
1442 of ADP:O ratios. *Methods Enzymol* 10:41-7. -
1443 www.mitoeagle.org/index.php/Estabrook_1967_Methods_Enzymol
- 1444 Faber C, Zhu ZJ, Castellino S, Wagner DS, Brown RH, Peterson RA, Gates L, Barton J,
1445 Bickett M, Hagerty L, Kimbrough C, Sola M, Bailey D, Jordan H, Elangbam CS (2014)
1446 Cardiolipin profiles as a potential biomarker of mitochondrial health in diet-induced
1447 obese mice subjected to exercise, diet-restriction and ephedrine treatment. *J Appl*
1448 *Toxicol* 34:1122-9.
- 1449 Fell D (1997) *Understanding the control of metabolism*. Portland Press.
- 1450 Garlid KD, Beavis AD, Ratkje SK (1989) On the nature of ion leaks in energy-transducing
1451 membranes. *Biochim Biophys Acta* 976:109-20. -
1452 www.mitoeagle.org/index.php/Garlid_1989_Biochim_Biophys_Acta
- 1453 Garlid KD, Semrad C, Zinchenko V. Does redox slip contribute significantly to mitochondrial
1454 respiration? In: Schuster S, Rigoulet M, Ouhabi R, Mazat J-P, eds (1993) *Modern trends*
1455 *in biothermokinetics*. Plenum Press, New York, London:287-93.

- 1456 Gerö D, Szabo C (2016) Glucocorticoids suppress mitochondrial oxidant production via
1457 upregulation of uncoupling protein 2 in hyperglycemic endothelial cells. PLoS One
1458 11:e0154813.
- 1459 Gnaiger E. Efficiency and power strategies under hypoxia. Is low efficiency at high glycolytic
1460 ATP production a paradox? In: Surviving Hypoxia: Mechanisms of Control and
1461 Adaptation. Hochachka PW, Lutz PL, Sick T, Rosenthal M, Van den Thillart G, eds
1462 (1993a) CRC Press, Boca Raton, Ann Arbor, London, Tokyo:77-109. -
1463 www.mitoeagle.org/index.php/Gnaiger_1993_Hypoxia
- 1464 Gnaiger E (1993b) Nonequilibrium thermodynamics of energy transformations. Pure Appl
1465 Chem 65:1983-2002. - www.mitoeagle.org/index.php/Gnaiger_1993_Pure_Appl_Chem
- 1466 Gnaiger E (2001) Bioenergetics at low oxygen: dependence of respiration and
1467 phosphorylation on oxygen and adenosine diphosphate supply. Respir Physiol 128:277-
1468 97. - www.mitoeagle.org/index.php/Gnaiger_2001_Respir_Physiol
- 1469 Gnaiger E (2014) Mitochondrial pathways and respiratory control. An introduction to
1470 OXPHOS analysis. 4th ed. Mitochondr Physiol Network 19.12. Oroboros MiPNet
1471 Publications, Innsbruck:80 pp. -
1472 www.mitoeagle.org/index.php/Gnaiger_2014_MitoPathways
- 1473 Gnaiger E (2009) Capacity of oxidative phosphorylation in human skeletal muscle. New
1474 perspectives of mitochondrial physiology. Int J Biochem Cell Biol 41:1837-45. -
1475 www.mitoeagle.org/index.php/Gnaiger_2009_Int_J_Biochem_Cell_Biol
- 1476 Gnaiger E, Méndez G, Hand SC (2000) High phosphorylation efficiency and depression of
1477 uncoupled respiration in mitochondria under hypoxia. Proc Natl Acad Sci USA
1478 97:11080-5. -
1479 www.mitoeagle.org/index.php/Gnaiger_2000_Proc_Natl_Acad_Sci_U_S_A
- 1480 Greggio C, Jha P, Kulkarni SS, Lagarrigue S, Broskey NT, Boutant M, Wang X, Conde
1481 Alonso S, Ofori E, Auwerx J, Cantó C, Amati F (2017) Enhanced respiratory chain

- 1482 supercomplex formation in response to exercise in human skeletal muscle. *Cell Metab*
1483 25:301-11. - http://www.mitoeagle.org/index.php/Greggio_2017_Cell_Metab
- 1484 Hofstadter DR (1979) Gödel, Escher, Bach: An eternal golden braid. A metaphorical fugue on
1485 minds and machines in the spirit of Lewis Carroll. Harvester Press:499 pp. -
1486 www.mitoeagle.org/index.php/Hofstadter_1979_Harvester_Press
- 1487 Illaste A, Laasmaa M, Peterson P, Vendelin M (2012) Analysis of molecular movement
1488 reveals latticelike obstructions to diffusion in heart muscle cells. *Biophys J* 102:739-48.
1489 - PMID: 22385844
- 1490 Jasienski M, Bazzaz FA (1999) The fallacy of ratios and the testability of models in biology.
1491 *Oikos* 84:321-26.
- 1492 Jepihhina N, Beraud N, Sepp M, Birkedal R, Vendelin M (2011) Permeabilized rat
1493 cardiomyocyte response demonstrates intracellular origin of diffusion obstacles.
1494 *Biophys J* 101:2112-21. - PMID: 22067148
- 1495 Klepinin A, Ounpuu L, Guzun R, Chekulayev V, Timohhina N, Tepp K, Shevchuk I,
1496 Schlattner U, Kaambre T (2016) Simple oxygraphic analysis for the presence of
1497 adenylate kinase 1 and 2 in normal and tumor cells. *J Bioenerg Biomembr* 48:531-48. -
1498 http://www.mitoeagle.org/index.php/Klepinin_2016_J_Bioenerg_Biomembr
- 1499 Klingenberg M (2017) UCP1 - A sophisticated energy valve. *Biochimie* 134:19-27.
- 1500 Koit A, Shevchuk I, Ounpuu L, Klepinin A, Chekulayev V, Timohhina N, Tepp K, Puurand
1501 M, Truu L, Heck K, Valvere V, Guzun R, Kaambre T (2017) Mitochondrial respiration
1502 in human colorectal and breast cancer clinical material is regulated differently. *Oxid*
1503 *Med Cell Longev* 1372640. -
1504 http://www.mitoeagle.org/index.php/Koit_2017_Oxid_Med_Cell_Longev
- 1505 Komlódi T, Tretter L (2017) Methylene blue stimulates substrate-level phosphorylation
1506 catalysed by succinyl-CoA ligase in the citric acid cycle. *Neuropharmacology* 123:287-
1507 98. - www.mitoeagle.org/index.php/Komlodi_2017_Neuropharmacology

- 1508 Lane N (2005) Power, sex, suicide: Mitochondria and the meaning of life. Oxford University
1509 Press:354 pp.
- 1510 Larsen S, Nielsen J, Neigaard Nielsen C, Nielsen LB, Wibrand F, Stride N, Schroder HD,
1511 Boushel RC, Helge JW, Dela F, Hey-Mogensen M (2012) Biomarkers of mitochondrial
1512 content in skeletal muscle of healthy young human subjects. J Physiol 590:3349-60. -
1513 http://www.mitoeagle.org/index.php/Larsen_2012_J_Physiol
- 1514 Lee C, Zeng J, Drew BG, Sallam T, Martin-Montalvo A, Wan J, Kim SJ, Mehta H, Hevener
1515 AL, de Cabo R, Cohen P (2015) The mitochondrial-derived peptide MOTS-c promotes
1516 metabolic homeostasis and reduces obesity and insulin resistance. Cell Metab 21:443-
1517 54.
- 1518 Lee SR, Kim HK, Song IS, Youm J, Dizon LA, Jeong SH, Ko TH, Heo HJ, Ko KS, Rhee BD,
1519 Kim N, Han J (2013) Glucocorticoids and their receptors: insights into specific roles in
1520 mitochondria. Prog Biophys Mol Biol 112:44-54.
- 1521 Leek BT, Mudaliar SR, Henry R, Mathieu-Costello O, Richardson RS (2001) Effect of acute
1522 exercise on citrate synthase activity in untrained and trained human skeletal muscle. Am
1523 J Physiol Regul Integr Comp Physiol 280:R441-7.
- 1524 Lemieux H, Blier PU, Gnaiger E (2017) Remodeling pathway control of mitochondrial
1525 respiratory capacity by temperature in mouse heart: electron flow through the Q-
1526 junction in permeabilized fibers. Sci Rep 7:2840. -
1527 www.mitoeagle.org/index.php/Lemieux_2017_Sci_Rep
- 1528 Lenaz G, Tioli G, Falasca AI, Genova ML (2017) Respiratory supercomplexes in
1529 mitochondria. In: Mechanisms of primary energy trasduction in biology. M Wikstrom
1530 (ed) Royal Society of Chemistry Publishing, London, UK:296-337.
- 1531 Margulis L (1970) Origin of eukaryotic cells. New Haven: Yale University Press.
- 1532 Meinild Lundby AK, Jacobs RA, Gehrig S, de Leur J, Hauser M, Bonne TC, Flück D,
1533 Dandanell S, Kirk N, Kaech A, Ziegler U, Larsen S, Lundby C (2017) Exercise training

- 1534 increases skeletal muscle mitochondrial volume density by enlargement of existing
1535 mitochondria and not de novo biogenesis. *Acta Physiol (Oxf)* [Epub ahead of print].
- 1536 Menshikova EV, Ritov VB, Fairfull L, Ferrell RE, Kelley DE, Goodpaster BH (2006) Effects
1537 of exercise on mitochondrial content and function in aging human skeletal muscle. *J*
1538 *Gerontol A Biol Sci Med Sci* 61:534-40.
- 1539 Menshikova EV, Ritov VB, Ferrell RE, Azuma K, Goodpaster BH, Kelley DE (2007)
1540 Characteristics of skeletal muscle mitochondrial biogenesis induced by moderate-
1541 intensity exercise and weight loss in obesity. *J Appl Physiol* (1985) 103:21-7.
- 1542 Menshikova EV, Ritov VB, Toledo FG, Ferrell RE, Goodpaster BH, Kelley DE (2005)
1543 Effects of weight loss and physical activity on skeletal muscle mitochondrial function in
1544 obesity. *Am J Physiol Endocrinol Metab* 288:E818-25.
- 1545 Miller GA (1991) *The science of words*. Scientific American Library New York:276 pp. -
1546 www.mitoeagle.org/index.php/Miller_1991_Scientific_American_Library
- 1547 Mitchell P (1961) Coupling of phosphorylation to electron and hydrogen transfer by a chemi-
1548 osmotic type of mechanism. *Nature* 191:144-8. -
1549 http://www.mitoglobal.org/index.php/Mitchell_1961_Nature
- 1550 Mitchell P (2011) Chemiosmotic coupling in oxidative and photosynthetic phosphorylation.
1551 *Biochim Biophys Acta Bioenergetics* 1807:1507-38. -
1552 <http://www.sciencedirect.com/science/article/pii/S0005272811002283>
- 1553 Mitchell P, Moyle J (1967) Respiration-driven proton translocation in rat liver mitochondria.
1554 *Biochem J* 105:1147-62. - www.mitoeagle.org/index.php/Mitchell_1967_Biochem_J
- 1555 Mogensen M, Sahlin K, Fernström M, Glinborg D, Vind BF, Beck-Nielsen H, Højlund K
1556 (2007) Mitochondrial respiration is decreased in skeletal muscle of patients with type 2
1557 diabetes. *Diabetes* 56:1592-9.
- 1558 Moreno M, Giacco A, Di Munno C, Goglia F (2017) Direct and rapid effects of 3,5-diiodo-L-
1559 thyronine (T2). *Mol Cell Endocrinol* 7207:30092-8.

- 1560 Morrow RM, Picard M, Derbeneva O, Leipzig J, McManus MJ, Gouspillou G, Barbat-Artigas
1561 S, Dos Santos C, Hepple RT, Murdock DG, Wallace DC (2017) Mitochondrial energy
1562 deficiency leads to hyperproliferation of skeletal muscle mitochondria and enhanced
1563 insulin sensitivity. *Proc Natl Acad Sci U S A* 114:2705-10. -
1564 www.mitoeagle.org/index.php/Morrow_2017_Proc_Natl_Acad_Sci_U_S_A
- 1565 Nicholls DG, Ferguson S (2013) *Bioenergetics* 4. Elsevier.
- 1566 Paradies G, Paradies V, De Benedictis V, Ruggiero FM, Petrosillo G (2014) Functional role
1567 of cardiolipin in mitochondrial bioenergetics. *Biochim Biophys Acta* 1837:408-17. -
1568 http://www.mitoeagle.org/index.php/Paradies_2014_Biochim_Biophys_Acta
- 1569 Pesta D, Hoppel F, Macek C, Messner H, Faulhaber M, Kobel C, Parson W, Burtscher M,
1570 Schocke M, Gnaiger E (2011) Similar qualitative and quantitative changes of
1571 mitochondrial respiration following strength and endurance training in normoxia and
1572 hypoxia in sedentary humans. *Am J Physiol Regul Integr Comp Physiol* 301:R1078–87.
- 1573 Price TM, Dai Q (2015) The role of a mitochondrial progesterone receptor (PR-M) in
1574 progesterone action. *Semin Reprod Med* 33:185-94.
- 1575 Prigogine I (1967) *Introduction to thermodynamics of irreversible processes*. Interscience,
1576 New York, 3rd ed:147pp.
- 1577 Puchowicz MA, Varnes ME, Cohen BH, Friedman NR, Kerr DS, Hoppel CL (2004)
1578 Oxidative phosphorylation analysis: assessing the integrated functional activity of
1579 human skeletal muscle mitochondria – case studies. *Mitochondrion* 4:377-85. -
1580 www.mitoeagle.org/index.php/Puchowicz_2004_Mitochondrion
- 1581 Puntschart A, Claassen H, Jostarndt K, Hoppeler H, Billeter R (1995) mRNAs of enzymes
1582 involved in energy metabolism and mtDNA are increased in endurance-trained athletes.
1583 *Am J Physiol* 269:C619-25.
- 1584 Quiros PM, Mottis A, Auwerx J (2016) Mitonuclear communication in homeostasis and
1585 stress. *Nat Rev Mol Cell Biol* 17:213-26.

- 1586 Reichmann H, Hoppeler H, Mathieu-Costello O, von Bergen F, Pette D (1985) Biochemical
1587 and ultrastructural changes of skeletal muscle mitochondria after chronic electrical
1588 stimulation in rabbits. *Pflugers Arch* 404:1-9.
- 1589 Renner K, Amberger A, Konwalinka G, Gnaiger E (2003) Changes of mitochondrial
1590 respiration, mitochondrial content and cell size after induction of apoptosis in leukemia
1591 cells. *Biochim Biophys Acta* 1642:115-23. -
1592 www.mitoeagle.org/index.php/Renner_2003_Biochim_Biophys_Acta
- 1593 Rich P (2003) Chemiosmotic coupling: The cost of living. *Nature* 421:583. -
1594 www.mitoeagle.org/index.php/Rich_2003_Nature
- 1595 Rostovtseva TK, Sheldon KL, Hassanzadeh E, Monge C, Saks V, Bezrukov SM, Sackett DL
1596 (2008) Tubulin binding blocks mitochondrial voltage-dependent anion channel and
1597 regulates respiration. *Proc Natl Acad Sci USA* 105:18746-51. -
1598 www.mitoeagle.org/index.php/Rostovtseva_2008_Proc_Natl_Acad_Sci_U_S_A
- 1599 Rustin P, Parfait B, Chretien D, Bourgeron T, Djouadi F, Bastin J, Rötig A, Munnich A
1600 (1996) Fluxes of nicotinamide adenine dinucleotides through mitochondrial membranes
1601 in human cultured cells. *J Biol Chem* 271:14785-90.
- 1602 Saks VA, Veksler VI, Kuznetsov AV, Kay L, Sikk P, Tiivel T, Tranqui L, Olivares J, Winkler
1603 K, Wiedemann F, Kunz WS (1998) Permeabilised cell and skinned fiber techniques in
1604 studies of mitochondrial function in vivo. *Mol Cell Biochem* 184:81-100. -
1605 http://www.mitoeagle.org/index.php/Saks_1998_Mol_Cell_Biochem
- 1606 Salabei JK, Gibb AA, Hill BG (2014) Comprehensive measurement of respiratory activity in
1607 permeabilized cells using extracellular flux analysis. *Nat Protoc* 9:421-38.
- 1608 Sazanov LA (2015) A giant molecular proton pump: structure and mechanism of respiratory
1609 complex I. *Nat Rev Mol Cell Biol* 16:375-88. -
1610 www.mitoeagle.org/index.php/Sazanov_2015_Nat_Rev_Mol_Cell_Biol

- 1611 Schneider TD (2006) Claude Shannon: biologist. The founder of information theory used
1612 biology to formulate the channel capacity. *IEEE Eng Med Biol Mag* 25:30-3.
- 1613 Schönfeld P, Dymkowska D, Wojtczak L (2009) Acyl-CoA-induced generation of reactive
1614 oxygen species in mitochondrial preparations is due to the presence of peroxisomes.
1615 *Free Radic Biol Med* 47:503-9.
- 1616 Schrödinger E (1944) *What is life? The physical aspect of the living cell*. Cambridge Univ
1617 Press. - www.mitoeagle.org/index.php/Gnaiger_1994_BTK
- 1618 Schultz J, Wiesner RJ (2000) Proliferation of mitochondria in chronically stimulated rabbit
1619 skeletal muscle--transcription of mitochondrial genes and copy number of
1620 mitochondrial DNA. *J Bioenerg Biomembr* 32:627-34.
- 1621 Simson P, Jepihhina N, Laasmaa M, Peterson P, Birkedal R, Vendelin M (2016) Restricted
1622 ADP movement in cardiomyocytes: Cytosolic diffusion obstacles are complemented
1623 with a small number of open mitochondrial voltage-dependent anion channels. *J Mol*
1624 *Cell Cardiol* 97:197-203. - PMID: 27261153
- 1625 Stucki JW, Ineichen EA (1974) Energy dissipation by calcium recycling and the efficiency of
1626 calcium transport in rat-liver mitochondria. *Eur J Biochem* 48:365-75.
- 1627 Tonkonogi M, Harris B, Sahlin K (1997) Increased activity of citrate synthase in human
1628 skeletal muscle after a single bout of prolonged exercise. *Acta Physiol Scand* 161:435-
1629 6.
- 1630 Waczulikova I, Habodaszova D, Cagalinec M, Ferko M, Ulicna O, Mateasik A, Sikurova L,
1631 Ziegelhöffer A (2007) Mitochondrial membrane fluidity, potential, and calcium
1632 transients in the myocardium from acute diabetic rats. *Can J Physiol Pharmacol* 85:372-
1633 81.
- 1634 Wagner BA, Venkataraman S, Buettner GR (2011) The rate of oxygen utilization by cells.
1635 *Free Radic Biol Med* 51:700-712. -
1636 <http://dx.doi.org/10.1016/j.freeradbiomed.2011.05.024> PMID: PMC3147247

- 1637 Wang H, Hiatt WR, Barstow TJ, Brass EP (1999) Relationships between muscle
1638 mitochondrial DNA content, mitochondrial enzyme activity and oxidative capacity in
1639 man: alterations with disease. *Eur J Appl Physiol Occup Physiol* 80:22-7.
- 1640 Wang T (2010) Coulomb force as an entropic force. *Phys Rev D* 81:104045. -
1641 www.mitoeagle.org/index.php/Wang_2010_Phys_Rev_D
- 1642 Watt IN, Montgomery MG, Runswick MJ, Leslie AG, Walker JE (2010) Bioenergetic cost of
1643 making an adenosine triphosphate molecule in animal mitochondria. *Proc Natl Acad Sci*
1644 *U S A* 107:16823-7. -
1645 www.mitoeagle.org/index.php/Watt_2010_Proc_Natl_Acad_Sci_U_S_A
- 1646 Weibel ER, Hoppeler H (2005) Exercise-induced maximal metabolic rate scales with muscle
1647 aerobic capacity. *J Exp Biol* 208:1635–44.
- 1648 White DJ, Wolff JN, Pierson M, Gemmell NJ (2008) Revealing the hidden complexities of
1649 mtDNA inheritance. *Mol Ecol* 17:4925–42.
- 1650 Wikström M, Hummer G (2012) Stoichiometry of proton translocation by respiratory
1651 complex I and its mechanistic implications. *Proc Natl Acad Sci U S A* 109:4431-6. -
1652 www.mitoeagle.org/index.php/Wikstroem_2012_Proc_Natl_Acad_Sci_U_S_A
- 1653 Willis WT, Jackman MR, Messer JI, Kuzmiak-Glancy S, Glancy B (2016) A simple hydraulic
1654 analog model of oxidative phosphorylation. *Med Sci Sports Exerc* 48:990-1000.